RESEARCH MEMORANDUM

A COMPARISON OF THE CALCULATED MAXIMUM-MANEUVER RESPONSE CHARACTERISTICS OF THREE AIR-TO-AIR, BEAM-RIDER, GUIDED MISSILES HAVING DIFFERENT LIFT RATIOS

By Howard F. Matthews and Elwood C. Stewart

Ames Aeronautical Laboratory
Moffett Field, Calif.

NATIONAL ADVISORY COMMITTEE
FOR AERONAUTICS

WASHINGTON
September 25, 1951

Classification cancelled (or changed to) UNCLASSIFIED

By Authority of NASA Tech Pub Announcement #24
(OFFICER AUTHORIZED TO CHANGE)

By 14057
NAME AND

NMB
GRADE OF OFFICER MAKING CHANGE)

30 Apr 64
DATE

NATIONAL ADVISORY COMMITTEE FOR AERONAUTICS

RESEARCH MEMORANDUM

A COMPARISON OF THE CALCULATED MAXIMUM-MANEUVER RESPONSE CHARACTERISTICS OF THREE AIR-TO-AIR, BEAM-RIDER, GUIDED MISSILES HAVING DIFFERENT LIFT RATIOS

By Howard F. Matthews and Elwood C. Stewart

SUMMARY

A comparison was made of the calculated response characteristics corresponding to the maximum maneuver of a variable-incidence, a canard, and a conventional tail-aft-control, beam-rider, guided missile, which are indicative, respectively, of a high positive, a low positive, and a negative lift ratio (the proportion of the lift developed by the movable control-surface deflection to the total lift in steady acceleration). All three configurations were designed to have the same weight, moment of inertia, and natural frequency, and to provide the same steady normal acceleration at identical angles of attack of the surface for which this angle is maximum. Differences in the response characteristics, therefore, represent primarily the effects of changes in lift ratio.

The results showed that for essentially the same practical limitations of normal acceleration and of the peak angle of attack of the surface which has the maximum angle of attack, the normal-displacement performance of the variable-incidence configuration is equal to or slightly better than that of the canard, depending on the type of guidance or control system used; and the performances of both are better than that of the conventional tail-aft-control missile. Consideration of additional factors such as servo energy, control-deflection interference limit, etc., may, in an over-all evaluation, outweigh the small decrease in normal-displacement response times associated with the higher positive lift ratios. In all cases the displacement performances are limited primarily by the aerodynamic rather than the guidance and stabilization-system characteristics.

INTRODUCTION

In the design of a missile intended to intercept and destroy maneuvering targets, it becomes necessary to select a value of the lift ratio, defined as the ratio of the lift developed by the movable control-surface deflection to the total lift at the design condition. If the remaining design requirements are assumed identical insofar as possible, differences in the lift ratio determine differences in the geometry of the missile; that is, whether the configuration will be a variable-incidence, a canard, or a conventional tail-aft-control missile. It is desirable, therefore, to have some concept of the relative response characteristics associated with changes in lift ratio before making a selection of this important quantity. Others (references 1, 2, 3, and 4) have made somewhat similar investigations, but have not considered the performance in terms of the spatial response nor have given any consideration to the possible effects of the guidance and stabilization system. Since the relation between the lethal radius of the warhead and the target-to-missile normal displacement at the time of conjunction is a measure of the effectiveness of a missile, it is the purpose of this paper to investigate and compare the effects of changes in lift ratio primarily in terms of relative normal displacement. Three widely different values of lift ratio were assumed so as to obtain a configuration of each of the three types of missiles. In addition, a beam-rider guidance system was chosen employing an error-lead network and a pitch-angle feedback stabilization system.

As a preliminary step in this investigation the design considerations involved in the aerodynamics and control system are discussed and criteria on which to base a comparison of the missile performances are established. As will be shown, there are several types of control systems that may be used in conjunction with the missiles, two of which are included in this report. The first system limits the control-surface deflection, while the second limits the angle of attack of the surface which has the largest angle of attack. Both analytical studies and differential-analyzer solutions are given for the comparison between missiles with each type of control system. Certain additional aspects are noted which are indicated by the results of this study and must be considered in an over-all comparison.

DEFINITIONS AND SYMBOLS

Critical surface: That surface which has the largest angle of attack at the trim condition

Maximum maneuver: The maneuver of the missile which utilizes the maximum capabilities of the missile

Interval: The time during which the control-surface deflection is at its limited value
(For the control systems discussed herein the first and second intervals refer to the time during which the surface deflection is limited at positive and negative values, respectively, for positive lift-ratio missiles and vice versa for negative lift-ratio missiles.)

Deadbeat response: A normal displacement response of the missile in which there is no overshoot above the center of the radar beam for a step displacement of the beam

Design condition: The Mach number and pressure altitude at which the missile design requirements are fixed

E_L output of error lead-network limiter, volts

E_{LN} output of error lead network, volts

E_p output of pitch-angle feedback circuit, volts

I_y moment of inertia, slug-feet squared

K_1 reciprocal gearing of servo, volts per radian

K_2 gearing of the radar, amplifier, and lead network, volts per foot

K_3 gearing of pitch-angle feedback circuit, volts per radian per second

K_g steady value of $\frac{\alpha}{\delta}$

L lift, pounds

M moment, foot-pounds

R ratio of lift developed by the movable control-surface deflection to the total lift at steady acceleration

$$\left[\frac{L_\delta \delta}{(L_\delta \delta + L_\alpha \alpha)} \right]$$

[redacted]

S	exposed surface area in one plane, feet squared
T_1	servo time lag, seconds
T_2, T_3, T_4, T_5	time constants of guidance and stabilization circuits, seconds
T_a, T_b, T_m, T_r	missile aerodynamic time constants, seconds
T_s^2	missile aerodynamic constant, radian-seconds squared per foot
V	missile velocity, feet per second
Y	transfer function
Z_B	normal displacement of radar beam from reference, feet
$\overline{Z}_B$	step magnitude of Z_B
Z_M	normal displacement of missile from reference, feet
b	semispan of wing, feet
c	local chord, feet
$\overline{c}$	mean aerodynamic chord $\left(\dfrac{\int_0^{b/2} c^2 dy}{\int_0^{b/2} c\, dy} \right)$
g	acceleration of gravity, 32.2 feet per second squared
l	distance between center of gravity and center of pressure of surface in presence of body, feet
l_b	body length, feet
m	mass of missile, slugs
n	steady normal acceleration factor $\left(\dfrac{\ddot{Z}_{M_{ss}}}{32.2} \right)$

p	a complex variable introduced in the Laplace transformation
r	lethal radius of warhead (assumed to be 15 feet)
t	time, seconds
t_m	miss time, seconds
y	spanwise station of local chord c, feet
α	angle of attack (fig. 1)
γ	flight path angle (fig. 1)
δ	control-surface deflection (fig. 1)
δ_L	limited control-surface deflection (fig. 2(a))
$\underline{\delta}$	control deflection for limited critical-surface angle of attack (fig. 2(b))
ζ_a, ζ_b	missile aerodynamic damping ratios
θ	angle of pitch (fig. 1) ($\theta = \alpha + \gamma$)

Subscripts

f	front surface
r	rear surface
ss	steady values at trim conditions

All angles are in radians unless otherwise noted. A ($\dot{}$) or ($\ddot{}$) above a symbol represents, respectively, the first or second derivative with respect to time. The symbols L_α, L_δ, M_α, ... represent $\frac{\partial L}{\partial \alpha}$, $\frac{\partial L}{\partial \delta}$, $\frac{\partial M}{\partial \alpha}$, ... etc. Other symbols used exclusively in the appendixes are defined therein.

PRELIMINARY CONSIDERATIONS

Transfer Functions

The simplified linearized equations for longitudinal motion referred to the axis system given in figure 1 are:

$$mV(\dot{\theta}-\dot{\alpha}) = L_\alpha\alpha + L_\delta\delta$$

$$I_y\ddot{\theta} = M_\alpha\alpha + M_\delta\delta + M_{\dot{\theta}}\dot{\theta} + M_{\dot{\alpha}}\dot{\alpha}$$

and the displacement equation is

$$\dot{Z}_M = V \sin\gamma \approx V\gamma$$

These and the lateral equations of motion are equivalent if the missile is roll stabilized, changes in forward speed are negligible, and the quantities are measured from trim condition.

The following aerodynamic transfer functions used in this study are derived in the usual manner from the above equations:

$$Y_\theta = \frac{\theta}{\delta} = \frac{(1+T_m p)}{VT_s^2 p(1+2\zeta_a T_a p+T_a^2 p^2)}$$

$$Y_Z = \frac{Z_M}{\theta} = \frac{V(1+2\zeta_b T_b p+T_b^2 p^2)}{p(1+T_m p)}$$

$$Y_\alpha = \frac{\alpha}{\delta} = \frac{K_g(1+T_r p)}{(1+2\zeta_a T_a p+T_a^2 p^2)}$$

where

$$T_a^2 = \frac{mVI_y}{-L_\alpha M_{\dot{\theta}}-mVM_\alpha} \approx \frac{-I_y}{M_\alpha} \qquad T_r = \frac{-L_\delta I_y}{L_\delta M_{\dot{\theta}}+mVM_\delta} \approx \frac{-L_\delta I_y}{mVM_\delta}$$

$$T_b^2 = \frac{L_\delta I_y}{L_\alpha M_\delta - L_\delta M_\alpha} \qquad K_g = \frac{L_\delta M_{\dot\theta} + mVM_\delta}{-L_\alpha M_{\dot\theta} - mVM_\alpha} \approx -\frac{M_\delta}{M_\alpha}$$

$$T_m = \frac{mVM_\delta - L_\delta M_{\dot\alpha}}{L_\alpha M_\delta - L_\delta M_\alpha} \approx \frac{mVM_\delta}{L_\alpha M_\delta - L_\delta M_\alpha} \qquad \zeta_a = \frac{L_\alpha I_y - mV(M_{\dot\theta} + M_{\dot\alpha})}{2\sqrt{mVI_y(-L_\alpha M_{\dot\theta} - mVM_\alpha)}}$$

$$T_s^2 = \frac{\frac{-L_\alpha M_{\dot\theta}}{V} - mM_\alpha}{L_\alpha M_\delta - L_\delta M_\alpha} \approx \frac{-mM_\alpha}{L_\alpha M_\delta - L_\delta M_\alpha} \qquad \zeta_b = \frac{-(M_{\dot\theta} + M_{\dot\alpha})}{2\sqrt{\frac{I_y}{L_\delta}(L_\alpha M_\delta - L_\delta M_\alpha)}}$$

The transfer functions of the guidance and stabilization system as shown in figure 2 are

Radar, amplifier and error-lead network $Y_L = \frac{K_2(1+T_4 p)}{(1+T_5 p)}$ Pitch-angle feedback $Y_p = \frac{K_3 p(1+T_2 p)}{(1+T_3 p)}$

Servo $Y_S = \frac{1}{K_1(1+T_1 p)}$

Aerodynamic Design

The aerodynamic performance requirements specified in common for each missile are

(a) 10g steady normal acceleration at a Mach number of 2.7 and a pressure altitude of 50,000 feet

(b) An angle of attack of the critical surface of approximately 20° for condition (a)
(This angle is $(\alpha + \delta)_{ss}$ for the variable-incidence and canard missiles and α_{ss} for the conventional tail-aft-control missile.)

(c) A missile natural frequency of approximately 2 cycles per second for condition (a)
(This value, along with I_y, uniquely determines the stability derivative M_α, since the damping is low and may be neglected.)

These requirements are considered typical of a supersonic, air-to-air, beam-rider, guided missile and arise in part from a consideration of the maximum maneuver (missile capture of the beam at the end of the boost phase of flight at the highest altitude), and the avoidance of excessive nonlinearity in the lift of the critical surface.

Three widely different values of lift ratio were selected to cover the three types of missiles. Along with a fifth design requirement, shown in the following table, the lift-ratio values are

Lift ratio	Missile	$\frac{l_f+l_r}{l_b}$
0.50	Variable incidence	0.45
.10	Canard	.66
-.24	Conventional tail aft control	.45

Assuming identical bodies, moments of inertia, weights, and wing plan forms, along with the five design requirements previously noted, the geometry of the variable-incidence and canard missiles and their stability derivatives may be determined in a manner similar to the method reported in reference 4. The $(\alpha/\delta)_{trim}$ appears to be of the correct order of magnitude for these two configurations. Results not presented herein showed that reasonable variations of $(\alpha/\delta)_{trim}$ will not significantly change the conclusions of the report. For the negative lift ratio, the stability derivative L_α is uniquely determined by a selection of the tail length l_r if the body geometric characteristics are assumed. An iterative process is then applied to determine the size of surfaces and the remaining stability derivatives. A summary of these assumed and computed characteristics is tabulated in table I.

Stabilization System

All beam-rider guidance systems, which utilize only an error detector and a servo to control the missile, are inherently unstable. Many methods of stabilization are possible and in this instance an error-lead network and a pitch-angle feedback circuit, which utilizes a lead network and ideal rate characteristics, were used. A block diagram of this system is shown in figure 2. The gearings and the error-lead

network design were initially based on an assumed linear system and the requirement that the steady displacement lag of the missile due to a beam accelerating at the design acceleration must not exceed the lethal radius of the warhead. The determination of the time constants for the pitch-angle feedback circuit was based on a compromise between the missile normal-displacement and control-deflection responses. However, preliminary studies indicated excessive normal accelerations and control deflections for a step displacement of the beam. A number of methods were available for reducing these values to reasonable magnitudes and the use of control-surface deflection limiters was selected because of certain advantages. The inclusion of these limiters separates the control of the missile by the stabilization system into two phases: a nonlinear portion during which the limiters are in operation and, as is shown later, controlled primarily by the lead-network time constants; and a linear phase. Two methods of control-surface limiting were used and are discussed later in the report. An additional limiter representing the radar saturation is also shown in figure 2.

COMPARISON CRITERIA

For a comparison of the performance of the three missiles with each type of control system, a 100-foot step displacement of the beam was chosen as it appeared to require a maneuver which is likely to be encountered during beam capture after boost or during flight. The criterion for comparing the responses of the three systems under consideration will be miss time, defined as the time during which the missile is beyond the assumed lethal radius. Miss time is directly related to the effectiveness in obtaining a hit if it is assumed that the target will not be passed before the missile has arrived within a lethal radius distance from the beam center. The performance of missiles, as indicated by the miss times, can also be compared in terms of other closely related criteria, such as: first, the miss range, that is, the range necessary to arrive within the lethal radius; or second, the distance that a missile is beyond the lethal radius when the missile with the best response is just at the lethal radius. Differences in miss ranges mean that in the case of beam capture the minimum launching ranges will differ, or, in the case of a disturbance during flight, the ineffective portions of the flight will vary.

It has been indicated previously that the missiles will be compared on the basis of two types of control-system limiting. The first method, in which the control-surface deflection is limited to produce the design steady acceleration, is a simple and practical means of reducing the magnitude of the normal acceleration associated with a step displacement of the beam. The second method, in which the angle of attack of the critical surface is limited, provides a comparison based on conditions which allow the maximum performance of each missile to be approached.

[redacted]

ANALYSIS, RESULTS AND DISCUSSION

Limited Control-Surface Deflection

Analytical study.- Analytical methods for determining the optimum response of a complex system appear to be impractical. Considerable simplification in the problem results, however, by introducing an assumed optimum control system which will cause the missile to reach the beam in the smallest miss time without regard for satisfying certain practical considerations, such as peak normal acceleration and peak critical-surface angle of attack. It is apparent that this can be accomplished by accelerating toward the beam with maximum capabilities for a certain time, then decelerating with maximum capabilities, followed by zero acceleration in order to remain on the beam. For this purpose, with the control-surface deflection limited as previously described, the optimum control system requires the surface deflection to be in the form of a square wave. The first and second intervals of this wave must be chosen to have the proper duration to minimize the miss time and hence define the optimum path.

It is possible to study the square-wave response, and therefore the optimum path, by studying only the step response since one cycle of a square wave can be decomposed into three steps as illustrated in figure 3. Although the exact expression for the step responses are complicated, it is shown later (p. 11 and appendix A) that the responses for all three missiles can be suitably simplified to

$$Z_M \approx \frac{ng}{2} t^2$$

where n is the steady acceleration factor corresponding to the step surface deflection. This result shows clearly that with the optimum control system the displacement response is limited by the aerodynamic design and that the three missiles should produce closely the same step responses since they are all designed to the same steady acceleration.

It is of interest to examine the nature of the optimum path in reaching the beam. Each step of the surface deflection in figure 3 produces its corresponding response, the resultant missile position being the sum of the three step responses. It is necessary that the two intervals of surface deflection be equal (or each a half period) and of a duration which will produce an optimum path by causing the overshoot above the beam center to equal the lethal radius as demonstrated in appendix B. The resultant miss time for the optimum system then becomes

$$t_m \approx \frac{2}{\sqrt{ng}} \left(\sqrt{Z_B + r} - \sqrt{r} \right)$$

which, when applied to the conditions of this comparison, gives $t_m = 0.763$ second for all three missiles. This value which is based on the approximate missile response equation (A10), $Z_M \approx \frac{ng}{2} t^2$, was found to be within 1 percent of the correct value from equation (A4) and hence justifies the use of the approximate equation. It can be reasoned that if the missile effective displacement frequency (equal to the reciprocal of twice the time for the missile to overshoot the beam by the lethal radius or equal to four times the half period) is much less than the missile natural frequency, sufficient time is available for the development of body angle of attack, and therefore differences in lift ratio are not important. For the conditions in this study, the effective displacement frequency is 0.416 cycles per second as compared to a 2.05 cps missile natural frequency. Since the pitching motion is oscillatory, however, the peaks of normal acceleration and critical-surface angle of attack require examination. The complete derivations of these quantities will be found in appendixes C and D, where it is shown that peak values occur in both the first and second half periods of the control-surface square-wave motion. The peak values as computed from these equations are given for each missile in the following table:

Lift ratio	Missile	Peak normal acceleration $\left(\frac{\ddot{Z}_M}{32.2}, g\right)$		Peak critical-surface angle of attack (deg)		Miss time (sec)
		Half period		Half period		
		1	2	1	2	
0.50	Variable incidence	14.2	−18.3	25.5	−30.4	0.763
.10	Canard	17.2	−24.1	29.1	−37.3	.763
−.24	Conventional tail aft control	20.9	−32.0	38.4	−57.0	.763

[redacted]

From the preceding table a comparison of the three missiles during the same half period indicates that the lower lift ratios produce higher peak values. It appears that these peaks may be excessive in relation to the design steady-state values for the canard missile and certainly so for the conventional tail-aft-control configuration. If the variable-incidence missile had been designed for a steady critical-surface angle of attack which would just produce the maximum permissible peak angle, the transient peak angles for the other missiles would be unsatisfactory. For a practical missile, a reduction of these peaks to satisfactory values could be accomplished by prescribing the surface deflection to be other than the perfect square wave as has been assumed. This means that since the lower lift-ratio missiles have larger peak values, a greater sacrifice must be made in the displacement response of the lower lift-ratio missiles by causing the surface deflection to depart farther from a square wave. It is apparent, then, that although all three missiles have the same optimum displacement performance, consideration of the other significant factors noted above indicates that the performance of the variable-incidence missile is best, followed in order by the canard and conventional tail-aft-control missile.

REAC solution.- In addition to the analytical study, an investigation was made on the Ames Reeves Electronic Analogue Computer (REAC) to find the magnitude of the deterioration in displacement response of the canard and conventional tail-aft-control configurations when the peak values of critical-surface angle of attack and acceleration were reduced to values approximating those of the variable-incidence missile. Values of the control-system parameters were varied in an exploratory manner so as to obtain an optimum path by making the first overshoot equal to the lethal radius. The two time constants in the error-lead network are the most effective in causing an optimum path, as shown in appendix E; thus, simplification of this procedure was permitted. The results for the three missiles are shown in figure 4. It should be noted that since the control deflection of the variable-incidence missile as given in figure 4(a) closely approaches the optimum square wave, the missile performance agrees well with the calculated values of the optimum system. A comparison of the results of figures 4(a) and 4(b) indicates that the displacement performance of the canard missile is somewhat poorer than that of the variable-incidence missile (0.023 second greater miss time), while the response of the conventional tail-aft-control missile in figure 4(c) shows a further increase in miss time (0.051 second greater than for the canard). Although it was found infeasible to make all peak values of critical-surface angle of attack and normal acceleration identical, additional data which are not presented indicated that the effect of these differences on the miss time would not significantly change the results. Therefore, as was indicated by the analytical study, it appears that for the type of control system assumed, the best performance is associated with the highest positive lift ratios. It is evident also that this is due to the necessary sacrifice in the normal-displacement

response caused by an increasing departure from the optimum square wave of control deflection in order to reduce the high peak critical angle of attack and acceleration associated with the lower lift ratios. Thus, the differences in displacement response are due basically to differences in missile characteristics and not in control-system characteristics. The important values relative to the motion of the three missiles as presented in figure 4 are summarized in the following table:

Lift ratio	Missile	Peak normal acceleration $\left(\frac{\ddot{z}_M}{32.2}, g\right)$		Peak critical-surface angle of attack (deg)		Miss time (sec)	Distance greater than lethal radius at time 0.797 second (ft)	Approximate increased miss range (ft)
		Half period		Half period				
		1	2	1	2			
0.50	Variable incidence	14.1	-17.4	25.3	-29.6	0.797	0	0
.10	Canard	17.0	-17.2	29.1	-29.7	.820	3	60
-.24	Conventional tail aft control	15.5	-12.1	27.0	-21.5	.871	10	195

The above conclusions also agree with those obtained from the deadbeat responses as can be seen from a comparison of the results of figure 5.

Limited Angle of Attack of the Critical Surface

Analytical study.– In an effort to obtain a response superior to that for the system in which the control-surface deflection is limited, it appeared that a control system which operated with a limited angle of attack of the critical surface would give better results. This objective is attained by deflecting the surface initially to this angle and thus additional gains can be realized from lift due to the increased control deflection and increased angular acceleration which develops lift due to angle of attack. The equations for the normal-displacement response to a step in the angle of attack of the critical surface are developed in appendix F in a manner similar to the procedure outlined previously. Here it is demonstrated that again the normal-displacement response is adequately represented by the formula

$$Z_M \approx \frac{ng}{2} t^2$$

where n is the steady normal-acceleration factor corresponding to a step steady critical angle of attack. Two significant conclusions may be drawn from this expression: first, since the peak permissible critical angle of attack is greater than the design steady-state value, a step in the critical-surface angle of attack with a magnitude equal to the peak permissible value will produce a greater steady acceleration with a resultant superior normal-displacement performance; and second, all three missiles will have the same normal-displacement performance if the optimum square wave in the critical angle of attack is followed. For the variable-incidence and canard missiles, the development of a square wave in the angle of attack of the critical surface $(\alpha + \delta)$ is theoretically obtainable. However, this is not possible for the conventional tail-aft-control missile due to the additional time lag necessary for the body and main lifting surface to turn to the angle of attack α of the critical surface. The conclusion, then, is that ideally the performance of the variable-incidence and canard missiles will be equal, with the conventional tail-aft-control missile being somewhat inferior.

REAC solution.– A square wave of critical angle of attack may be closely approached through the use of appropriate circuits. However, it can be obtained simply by means of an $(\alpha + \delta)$ limiter as illustrated in figure 2(b). The analogous block diagram for this system as used on the REAC is also given on figure 2(b). It should be noted in this figure that $\underline{\delta}$ is identical to δ if the limiting $(\alpha + \delta)$ is not reached. A factor which reduces the practicability of this sytem somewhat is the difficulty of obtaining accurate angle-of-attack measurements.

As mentioned previously, it is not possible to obtain a square wave in the critical angle of attack for the conventional tail-aft-control missile. A close approach to this condition is obtainable as can be seen in figure 6 for this missile. Although the peak positive and negative angles of attack are not identical, it was believed that with further exploration on the REAC an angle of 22° for both peaks could be obtained without a significant increase in miss time. For convenience, then, the limit of 22° was selected for the critical angle of attack of the other two missiles. The REAC results for the variable-incidence and canard missiles are shown in figures 6(a) and (b). It is apparent that the data from the REAC closely approaches the results indicated by the analytical study. These results are summarized in the following table:

Lift ratio	Missile	Miss time (sec)	Distance greater than lethal radius at t = 0.770 second (ft)	Approx-mate increased miss range (ft)
0.50	Variable incidence	0.770	0	0
.10	Canard	.789	2	50
−.24	Conventional tail aft control	.878	17	285

A comparison of the above data with that for the control system in which the surface deflection is limited confirms the superiority in performance of the system with limited critical-surface angle of attack. The reason the difference is not more marked is that the critical angle-of-attack limit was not set at the peak permissible value.

It should be noted that for this type of limiter the control-surface deflections of the variable-incidence missile exceed the interference limit of about 15° between the pitch and yaw controls. The effects of this interference limit are discussed in the next section.

[redacted]

ADDITIONAL DESIGN FACTORS

As is well known, the design of a missile is extremely complicated; in fact, it is difficult to give a definition of an optimum missile. Certain designers interpret the optimum missile to be one which meets the design conditions for the least cost. The factors which determine the over-all cost are many, but certainly the size of the components, the total exposed wing surface, storage, and ease of assembly considerations, etc., are important factors, a few of which are discussed in the following sections.

Servo Energy

It is possible to approximate the relative servo energy consumed in flight for the three missiles under consideration. A conventional hydraulic system employing a linear piston actuator with an accumulator is typical of servo systems used in air-to-air supersonic missiles (reference 5). For this type of system, the servo energy consumed is equal to the change in the product of the pressure and volume of oil in the accumulator and is approximately equal to the average pressure times the product of the gearing between the control deflection and servo-piston movement, the servo-piston area, and the sum of the absolute movements of the control surface between points at which $\dot{\delta}$ changes sign. The combination of the pressure, servo-piston size, and gearing is designed to meet the expected maximum hinge moment. If the same static margin of the control surface is used for each of the three missiles and it is assumed that the hinge-moment coefficient due to δ is equal to that due to α, the maximum hinge moment is directly proportional to the product of the exposed surface area S, its mean aerodynamic chord $\bar{c}$, and the design maximum angle of attack. By use of the actual maximum angle of attack of the control surface as given in the applicable time histories to represent the design maximum angle of attack, the relative consumption of servo energy is given by the ratio of this quantity times $S\bar{c}\Sigma|\delta|$ for any two of the missiles. The results for each missile based on the deadbeat response of the canard are given in the following table:

Lift ratio	Type response and limiter / Missile	Relative servo energy: Optimum; surface control deflection	Relative servo energy: Optimum; surface angle of attack	Relative servo energy: Deadbeat; surface control deflection
0.50	Variable incidence	7.7	12.3	6.1
.10	Canard	1.2	2.2	1.0
−.24	Conventional tail aft control	2.2	2.2	2.1

These ratios indicate that the variable-incidence missile requires a relatively large servo-energy storage capacity in relation to the other two configurations.

Surface-Deflection Interference

Another unfavorable factor associated with the variable-incidence configuration is the possible interference between the pitch and yaw control surfaces. For the control system using a surface deflection limiter, the interference limit for all three missiles was not exceeded, although this limit and the control-deflection limit are approximately equal for the variable-incidence configuration. Thus, for the higher ratios at the same design acceleration or for the same lift ratio at higher design accelerations, the variable-incidence missile becomes increasingly inefficient using the same plan form since the design surface angle of attack must be reduced and larger surface areas are necessary.

For the control system using a critical-surface angle-of-attack limiter, the interference limit of the control surfaces was exceeded by only the variable-incidence missile. From a consideration of this limitation, it is concluded that the normal-displacement performance of the variable-incidence missile may be somewhat poorer than that of the canard in this instance.

[redacted]

Size of Surfaces

A comparison of the total exposed surface areas indicates that the conventional tail-aft-control missile has the smallest area, while those for the other two configurations are nearly equal. It appears, then, that the range performance of this missile will be superior to the others at low lift coefficients. At higher lift coefficients, the relative range performance is uncertain without an investigation of the lift-drag ratios of the three missiles.

CONCLUDING REMARKS

A study has been made of the response characteristics to the maximum maneuver at the design condition of a variable-incidence, a canard, and a conventional tail-aft-control missile, which are indicative, respectively, of a high positive, a low positive, and a negative lift ratio. Since other design requirements for the three missiles have been assumed identical insofar as possible, the conclusions presented represent primarily the effects of changes in lift ratio.

For the control deflection limited to that value which will give the design steady acceleration, the optimum normal-displacement response is the same for all configurations. It can be reasoned that this is due to the missile effective displacement frequency being much less than the missile natural frequency, thus allowing sufficient time for the development of lift due to angle of attack; and, therefore, differences in lift ratio are not important. However, the angle of attack of the critical surface and the normal acceleration show increasing peak values with decreasing lift ratio due to pitching oscillations. A reduction in these peaks to satisfactory values can be made by an increasing sacrifice in the normal-displacement performance with decreasing lift ratio.

For the missiles compared on the basis of the same limited angle of attack of the critical surface, the theoretical optimum normal-displacement performance is again unchanged by the configuration. Since missiles with negative lift ratios cannot approach the theoretical optimum square wave of the critical angle of attack, the displacement performances of the variable-incidence and canard configurations, which are nearly equal, are superior to that of the conventional tail-aft-control missile as long as the interference limit between the pitch and yaw control surfaces is not reached.

Certain aspects, such as the servo energy storage required and the control interference limitations, favor the lower lift ratios. In an

over-all evaluation, these and other important factors as, for example, the ease of assembly, storage problems, effects of noise, etc., must be considered and may outweigh the small decrease in normal-displacement response time associated with the higher positive lift ratios.

The normal-displacement performances of all missiles discussed herein are primarily restricted by the aerodynamic rather than the guidance- and stabilization-system characteristics. In many instances involving missile control-system combinations it appears possible that preliminary studies may be simplified by eliminating details of the control system from consideration and by assuming that the missile is controlled by the desired surface deflection, since it is probable that a control system can be devised to produce reasonable desired deflections.

Ames Aeronautical Laboratory,
National Advisory Committee for Aeronautics,
Moffett Field, Calif.

[redacted]

APPENDIX A

MISSILE RESPONSE TO A STEP SURFACE DEFLECTION

The missile transfer function relating surface deflection to missile vertical position can be shown to be

$$\frac{Z_M}{\delta}(p) = \left[\frac{Z_M}{\theta}(p)\right]\left[\frac{\theta}{\delta}(p)\right]$$

$$= \frac{T_b^2 p^2 + 2\zeta_b T_b p + 1}{T_s^2 p^2 (T_a^2 p^2 + 2\zeta_a T_a p + 1)} \tag{A1}$$

The response for a step surface deflection of magnitude δ_L is then

$$Z_M(p) = \frac{\delta_L (T_b^2 p^2 + 2\zeta_b T_b p + 1)}{T_s^2 p^3 (T_a^2 p^2 + 2\zeta_a T_a p + 1)}$$

$$= \frac{\delta_L (T_b^2 p^2 + 2\zeta_b T_b p + 1)}{T_s^2 T_a^2 p^6 [p - (-\sigma_a + i\lambda_a)][p - (-\sigma_a - i\lambda_a)]} \tag{A2}$$

where

$$\sigma_a = \frac{\zeta_a}{T_a} \qquad \lambda_a = \frac{\sqrt{1 - \zeta_a^2}}{T_a}$$

In terms of a partial-fraction expansion,

$$Z_M(p) = \frac{a_0}{p} + \frac{a_1}{p^2} + \frac{a_2}{p^3} + \frac{a_3}{p - (-\sigma_a + i\lambda_a)} + \frac{\bar{a}_3}{p - (-\sigma_a - i\lambda_a)} \tag{A3}$$

where $\bar{a}_3$ is the complex conjugate of a_3. The residues can be found as follows:

$$a_0 = \frac{1}{2} \lim_{p \to 0} \left\{ \frac{d^2[p^3 Z_M(p)]}{dp^2} \right\} = \frac{\delta_L}{T_s^2}(T_b^2 - T_a^2 - 4\zeta_a T_a \zeta_b T_b + 4\zeta_a^2 T_a^2)$$

$$a_1 = \lim_{p \to 0} \left\{ \frac{d[p^3 Z_M(p)]}{dp} \right\} = \frac{2\delta_L}{T_s^2}(\zeta_b T_b - \zeta_a T_a)$$

$$a_2 = \lim_{p \to 0} [p^3 Z_M(p)] = \frac{\delta_L}{T_s^2}$$

$$a_3 = \lim_{p \to (-\sigma_a + i\lambda_a)} \left\{ [p - (-\sigma_a + i\lambda_a)]\, Z_M(p) \right\}$$

$$= \frac{\delta_L T_b^2}{2T_s^2 T_a^2} \times \frac{(\sigma_a^2 - \lambda_a^2 - 2\sigma_a\sigma_b + \sigma_b^2 + \lambda_b^2) + i(2\sigma_b\lambda_a - 2\sigma_a\lambda_a)}{(\lambda_a^4 - 3\sigma_a^2\lambda_a^2) + i(3\sigma_a\lambda_a^3 - \sigma_a^3\lambda_a)}$$

where σ_b and λ_b are defined in the same manner as for σ_a and λ_a, that is,

$$\sigma_b = \frac{\zeta_b}{T_b} \qquad \text{and} \qquad \lambda_b = \frac{\sqrt{1 - \zeta_b^2}}{T_b}$$

For all missiles under investigation $\lambda_a \gg \sigma_a$, $\lambda_b^2 - \lambda_a^2 \gg \sigma_a^2 + \sigma_b^2 - 2\sigma_a\sigma_b$, and $\lambda_b^2 - \lambda_a^2 \gg 6\sigma_a(\sigma_b - \sigma_a)$ so that a_3 reduces to

$$a_3 = \frac{\delta_L T_b}{2T_s^2} \frac{(\lambda_b^2 - \lambda_a^2) - i\left[3\sigma_a\left(\frac{\lambda_b^2 - \lambda_a^2}{\lambda_a}\right) + 2\lambda_a(\sigma_a - \sigma_b) \right]}{(\lambda_a^2 + 9\sigma_a^2)}$$

The time-history response can then be written as

$$Z_M(t) = a_0 + a_1 t + \frac{a_2}{2}t^2 + a_3 e^{(-\sigma_a + i\lambda_a)t} + \bar{a}_3 e^{(-\sigma_a - i\lambda_a)t}$$

$$= a_0 + a_1 t + \frac{a_2}{2}t^2 + 2\sqrt{a_{3R}^2 + a_{3I}^2}\, e^{-\sigma_a t} \cos\left(\lambda_a t + \tan^{-1}\frac{a_{3I}}{a_{3R}}\right)$$

$$= a_0 + a_1 t + \frac{a_2}{2}t^2 + a_4 e^{-\sigma_a t} \cos(\lambda_a t + \epsilon) \qquad \text{(A4)}$$

where a_{3R} and a_{3I} refer to the real and imaginary part of a_3. The correct phase angle must reduce Z_M to zero at time zero which means it must satisfy the equation $a_0 + a_4 \cos\epsilon = 0$.

The values of the coefficients in equation (A4), using parameters given in table II, are presented as follows:

Parameter	Variable incidence	Canard	Tail aft control
a_0	−0.94	−1.70	−2.37
a_1	−1.90	−3.30	−2.43
a_2	322	322	322
a_{3R}	.467	.849	1.18
a_{3I}	−.094	−.188	−.143
a_4	.95	1.74	2.38
ϵ	−11.4°	−12.5°	−6.9°

Hence the missile equations are:

$$\left.\begin{aligned}
&\text{Variable incidence} \quad Z_M(t) = -0.941 - 1.90t + 161t^2 + 0.95e^{-0.891t}\cos\,(739t-11.4)\\
&\text{Canard} \quad Z_M(t) = -1.70 - 3.30t + 161t^2 + 1.74e^{-0.917t}\cos\,(739t-12.5)\\
&\text{Tail aft control} \quad Z_M(t) = -2.37 - 2.43t + 161t^2 + 2.38e^{-0.547t}\cos\,(739t-6.9)
\end{aligned}\right\} \tag{A5}$$

It appears that for values of t greater than about 1/2 second, the above equations can be adequately approximated by the t^2 term in equation (A4) as

$$Z_M \approx \frac{\delta_L}{2T_s^2}\,t^2 \tag{A6}$$

The design ratio δ_L/T_s^2 can be simplified further in terms of the steady acceleration factor from the following simplified lift and moment equations at trim conditions:

$$L_{ss} = L_\delta \delta_L + L_\alpha \alpha_{ss}$$

$$M_\delta \delta_L + M_\alpha \alpha_{ss} = 0$$

The steady angle of attack α_{ss} corresponding to a surface deflection δ_L is, from the moment equation,

$$\alpha_{ss} = -\frac{M_\delta}{M_\alpha}\delta_L \tag{A7}$$

which substituted in the lift equation and solved for the value of δ_L gives

$$\delta_L = \frac{L_{ss}}{L_\delta - \frac{L_\alpha M_\delta}{M_\alpha}} \tag{A8}$$

Letting the steady lift be ngm, δ_L reduces to

$$\delta_L = \frac{ngm}{L_\delta - \frac{L_\alpha M_\delta}{M_\alpha}} = ngT_s^2 \tag{A9}$$

The missile response then becomes

$$Z_M \approx \frac{ng}{2} t^2 \tag{A10}$$

APPENDIX B

MISSILE RESPONSE FOR AN OPTIMUM STABILIZATION SYSTEM

The general discussion given in the section on limited control deflection and the information in figure 3 are applicable to the following study. For the first interval during which the deflection is positive

$$Z_M \approx \frac{ng}{2} t^2 \tag{B1}$$

During the second interval the deflection is negative, the missile response is composed of two t^2 functions displaced in time, one positive starting at time zero and the other negative of twice the magnitude beginning at the start of the second interval or at the switch time t_{s1}.

$$Z_M \approx \frac{ng}{2}t^2 - 2\left[\frac{ng}{2}(t-t_{s1})^2\right]$$

$$\approx ng\left[-\frac{t^2}{2} + 2tt_{s1} - t_{s1}^2\right] \tag{B2}$$

A maximum of this equation occurs when

$$\frac{dZ_M}{dt} \approx ng\left[-t + 2t_{s1}\right] = 0$$

or when $t \approx 2t_{s1}$. During the third interval in which the surface deflection is zero, the response is composed of the two t^2 functions discussed for the second interval in addition to a positive t^2 function beginning at the start of the third interval or at the switch time t_{s2}.

$$Z_M \approx \frac{ng}{2}t^2 - 2\left[\frac{ng}{2}(t-t_{s1})^2\right] + \frac{ng}{2}(t-t_{s2})^2$$

$$\approx ng\left[(2t_{s1}-t_{s2})t + \left(\frac{t_{s2}^2}{2} - t_{s1}^2\right)\right] \tag{B3}$$

To reach and remain on the beam at a constant value of Z_M it is easy to show that for

$$\frac{dZ_M}{dt} \approx ng\,(2t_{s1}-t_{s2}) = 0$$

it is necessary that $t_{s2} \approx 2t_{s1}$ which means that the first and second

intervals of the surface deflection are equal or each interval is a half period. It is necessary, in addition, to determine the required duration of the half periods so as to minimize the miss time. A qualitative examination of this problem indicates that for the optimum displacement response the overshoot above the beam center should equal the lethal radius. This conclusion has been mathematically verified. Equation (B2) evaluated at $t \approx 2t_{s1}$ expresses the missile position at the peak and for an optimum response this position must be $\bar{Z}_B + r$, giving

$$(Z_M)_{max} = \bar{Z}_B + r \approx ng\left(-\frac{t^2}{2} + 2t_{s1}t - t_{s1}^2\right)_{t=2t_{s1}}$$

A solution for t_{s1} then yields

$$t_{s1} \approx \sqrt{\frac{\bar{Z}_B + r}{ng}} \tag{B4}$$

For the conditions assumed, t_{s1} equals 0.60 second.

The magnitude of miss time for the optimum path can also be found from equation (B2) as the value of t which will bring the missile position to $\bar{Z}_B - r$.

$$Z_M = \bar{Z}_B - r \approx ng\left(-\frac{t_m^2}{2} + 2t_{s1}t_m - t_{s1}^2\right)$$

from which

$$t_m \approx \frac{2}{\sqrt{ng}}\left(\sqrt{\bar{Z}_B + r} - \sqrt{r}\right) \tag{B5}$$

Physical reasoning shows the minus sign to be correct. For the assumed conditions, t_m equals 0.763 second.

APPENDIX C

MISSILE ACCELERATION FOR AN OPTIMUM STABILIZATION SYSTEM

The acceleration of the missile when subjected to a square wave of surface deflection can be found from the response to a step, as has been described in detail for the determination of missile position. The transfer function relating surface deflection to normal acceleration is

$$\frac{\ddot{Z}_M}{\delta}(p) = \frac{(T_b^2p^2+2\zeta_bT_bp+1)}{T_s^2(T_a^2p^2+2\zeta_aT_ap+1)} \tag{C1}$$

For a step surface deflection of magnitude δ_L the response becomes

$$\ddot{Z}_M(p) = \frac{\delta_L(T_b^2p^2+2\zeta_bT_bp+1)}{T_s^2p(T_a^2p^2+2\zeta_aT_ap+1)}$$

$$= \frac{\delta_L(\sigma_a^2+\lambda_a^2)[p^2+2\sigma_bp+(\sigma_b^2+\lambda_b^2)]}{T_s^2(\sigma_b^2+\lambda_b^2)p[(p+\sigma_a)^2+\lambda_a^2]} \tag{C2}$$

where

$$\sigma_a = \frac{\zeta_a}{T_a} \qquad \sigma_b = \frac{\zeta_b}{T_b} \qquad \lambda_a = \frac{\sqrt{1-\zeta_a^2}}{T_a} \qquad \lambda_b = \frac{\sqrt{1-\zeta_b^2}}{T_b}$$

The time solution can be shown to be

$$\ddot{Z}_M(t) = \frac{\delta_L(\sigma_a^2+\lambda_a^2)}{T_s^2(\sigma_b^2+\lambda_b^2)}\left[\frac{\sigma_b^2+\lambda_b^2}{\sigma_a^2+\lambda_a^2} + \frac{\sqrt{(\sigma_a^2-\lambda_a^2-2\sigma_a\sigma_b+\sigma_b^2+\lambda_b^2)^2+\lambda_a^2(2\sigma_b-2\sigma_a)^2}}{\lambda_a\sqrt{\sigma_a^2+\lambda_a^2}}e^{-\sigma_at}\sin(\lambda_at+\psi_1+\rho_1)\right] \tag{C3}$$

where

$$\psi_1 = \tan^{-1}\frac{-2\lambda_a(\sigma_a-\sigma_b)}{\lambda_b^2-\lambda_a^2+\sigma_a^2+\sigma_b^2-2\sigma_a\sigma_b}$$

$$\rho_1 = \tan^{-1}\frac{\lambda_a}{\sigma_a}$$

This equation represents, of course, the acceleration throughout the first half period. It will be desirable to express the acceleration in the following form where, for purposes of satisfying the initial conditions, the sign of the second term has been changed to allow the use of the smallest of the multiple values for ψ_1 and ρ_1

$$\ddot{Z}_M(t) = b_o - b_1 e^{-\sigma_a t}\sin(\lambda_a t+\psi_1+\rho_1) \tag{C4}$$

$$b_o = \frac{\delta_L}{T_s^2}$$

$$b_1 = \frac{\delta_L\sqrt{\sigma_a^2+\lambda_a^2}\sqrt{(\sigma_a^2-\lambda_a^2-2\sigma_a\sigma_b+\sigma_b^2+\lambda_b^2)^2+\lambda_a^2(2\sigma_b-2\sigma_a)^2}}{T_s^2\,\lambda_a(\sigma_b^2+\lambda_b^2)}$$

Considerable simplification results from a consideration of relative magnitudes of the parameters. For all the missiles under discussion in this report, it is possible to show that $\lambda_a^2 \gg \sigma_a^2$, $\lambda_b^2-\lambda_a^2 \gg \sigma_a^2+\sigma_b^2-2\sigma_a\sigma_b$, and $\lambda_b^2-\lambda_a^2 \gg 4\lambda_a^2(\sigma_b-\sigma_a)^2$. Using primed values for approximate unprimed parameters, the solution is then

$$\ddot{Z}_M(t) \approx b_o - b_1' e^{-\sigma_a t}\sin(\lambda_a t+\psi_1'+\rho_1) \tag{C5}$$

where

$$b_1' = \frac{\delta_L T_b^2(\lambda_b^2-\lambda_a^2)}{T_s^2}$$

$$\psi_1' = \tan^{-1}\frac{-2\lambda_a(\sigma_a-\sigma_b)}{\lambda_b^2-\lambda_a^2}$$

For the second half period, the acceleration is expressible as

$$\ddot{Z}_M(t) = b_o-b_1e^{-\sigma_a t}\sin(\lambda_a t+\psi_1+\rho_1)-2\left\{b_o-b_1e^{-\sigma_a(t-t_{s1})}\sin[\lambda_a(t-t_{s1})+\psi_1+\rho_1]\right\}$$

$$= -b_o-b_1e^{-\sigma_a t}[\sin(\lambda_a t+\psi_1+\rho_1)-2e^{\sigma_a t_{s1}}\sin(\lambda_a t+\psi_1+\rho_1-\lambda_a t_{s1})]$$

$$= -b_o-b_1e^{-\sigma_a t}\sqrt{\eta^2+\Omega^2}\,\sin(\lambda_a t+\psi_1+\rho_1+\rho_2) \tag{C6}$$

where

$$\eta = 1-2e^{\sigma_a t_{s1}}\cos\lambda_a t_{s1} \qquad \Omega = 2e^{\sigma_a t_{s1}}\sin\lambda_a t_{s1} \qquad \rho_2 = \tan^{-1}\frac{\Omega}{\eta}$$

Simplification then gives

$$\ddot{Z}_M(t) \approx -b_o - b_1' e^{-\sigma_a t}\sqrt{\eta^2+\Omega^2}\sin(\lambda_a t+\psi_1'+\rho_1+\rho_2) \tag{C7}$$

The peak value in each of the two half periods is of primary interest. In the first half period it can be found by determining the value of time t_{x1} at which the peak occurs. The equation

$$\frac{d\ddot{Z}_M}{dt} = -b_1[\lambda_a e^{-\sigma_a t}\cos(\lambda_a t+\psi_1+\rho_1) - \sigma_a e^{-\sigma_a t}\sin(\lambda_a t+\psi_1+\rho_1)] = 0$$

can be satisfied only if

$$\lambda_a t + \psi_1 = n\pi \qquad n = 0, 1, 2, \ldots$$

or

$$t_{x1} = \frac{n\pi - \psi_1}{\lambda_a} \tag{C8}$$

The value of n must be chosen so that t_{x1} is approximately half way between zero and t_{s1}.

Then evaluating equation (C4) at t_{x1} gives

$$(\ddot{Z}_M)_{max} = b_o - b_1 e^{-\sigma_a t_{x1}}\sin\left(n\pi+\tan^{-1}\frac{\lambda_a}{\sigma_a}\right)$$

$$= b_o - b_1 e^{-\sigma_a t_{x1}}\sin\left(n\pi+\sin^{-1}\frac{\lambda_a}{\sqrt{\lambda_a^2+\sigma_a^2}}\right)$$

$$= b_o - (-1)^n b_1 e^{-\sigma_a t_{x1}}\frac{\lambda_a}{\sqrt{\lambda_a^2+\sigma_a^2}} \tag{C9}$$

which, according to the previous approximations, is

$$(\ddot{Z}_M)_{max} \approx b_o - (-1)^n b_1' e^{-\sigma_a t_{x1}}$$

Numerical calculations show that for the first interval $n = 1$ giving

$$(\ddot{Z})_{max} \approx b_o + b_1' e^{-\sigma_a t_{x1}} \tag{C10}$$

The second half period can be treated in a similar manner utilizing equation (C6). The value of time t_{x2} in this second half period can be found from

$$\frac{d\ddot{Z}_M}{dt} = -b_1\sqrt{\eta^2+\Omega^2}\left[\lambda_a e^{-\sigma_a t}\cos\left(\lambda_a t+\psi_1+\rho_1+\rho_2\right) - \sigma_a e^{-\sigma_a t}\sin\left(\lambda_a t+\psi_1+\rho_1+\rho_2\right)\right] = 0$$

which requires that

$$t_{x2} = \frac{n\pi - \psi_1 - \rho_2}{\lambda_a} \tag{C11}$$

Hence the peak value is

$$\left(\ddot{Z}_M\right)_{max} = -b_o - b_1 e^{-\sigma_a t_{x2}}\sqrt{\eta^2+\Omega^2}\,\sin\left(n\pi+\tan^{-1}\frac{\lambda_a}{\sigma_a}\right)$$

$$= -b_o - b_1 e^{-\sigma_a t_{x2}}\sqrt{\eta^2+\Omega^2}\,\sin\left(n\pi+\sin^{-1}\frac{\lambda_a}{\sqrt{\lambda_a^2+\sigma_a^2}}\right)$$

$$= -b_o - (-1)^n b_1 e^{-\sigma_a t_{x2}}\sqrt{\eta^2+\Omega^2}\,\frac{\lambda_a}{\sqrt{\lambda_a^2+\sigma_a^2}} \tag{C12}$$

Again using previously discussed approximations,

$$\left(\ddot{Z}_M\right)_{max} \approx -b_o - (-1)^n b_1'\sqrt{\eta^2+\Omega^2}\; e^{-\sigma_a t_{x2}}$$

For this interval calculations show that $n = 4$; thus,

$$\left(\ddot{Z}_M\right)_{max} \approx -b_o - b_1'\sqrt{\eta^2+\Omega^2}\; e^{-\sigma_a t_{x2}} \tag{C13}$$

Numerical substitution of missile parameters then gives the following values:

Parameter	Variable incidence	Canard	Tail aft control
b_o, fps^2	322	322	322
b_1', fps^2	159	290	400
t_{x1}, sec	.247	.244	.244
t_{x2}, sec	.872	.865	.855
η	.606	.550	.638
Ω	2.99	3.42	2.76
ρ_1, deg	86.9	85.9	87.6
ρ_2, deg	78.6	80.9	77.0
ψ_1', deg	−2.7	−.3	.4

[redacted]

The preceding values then give the following results for the time history and maximum values:

	Normal acceleration, $\ddot{Z}_M/g$	
	Time history	Maximum value
Half period 1		
Variable incidence	$10 - 4.94e^{-0.691t} \sin (739t+84.2)$	14.17
Canard	$10 - 9.00e^{-0.917t} \sin (739t+85.6)$	17.21
Tail aft control	$10 - 12.42e^{-0.547t} \sin (739t+88.0)$	20.90
Half period 2		
Variable incidence	$-10 - 15.05e^{-0.691t} \sin (739t+162.8)$	-18.27
Canard	$-10 - 31.20e^{-0.917t} \sin (739t+166.5)$	-24.10
Tail aft control	$-10 - 35.30e^{-0.547t} \sin (739t+165.0)$	-32.00

It is of interest to notice that the phase angles at the beginning of each half period are nearly $\pi/2$ so that the time-variant portion of the time histories approximates a damped cosine function as shown below:

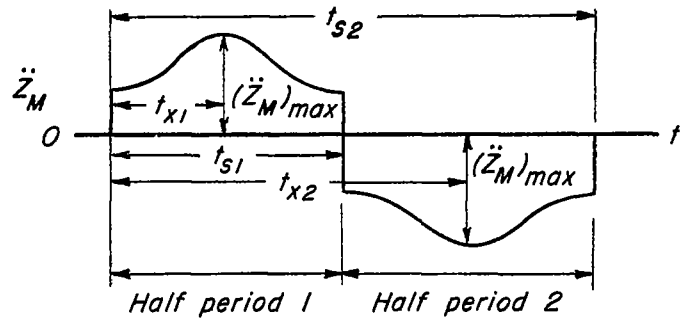

APPENDIX D

MISSILE CRITICAL ANGLE OF ATTACK FOR AN OPTIMUM STABILIZATION SYSTEM

The determination of the critical angle of attack follows very closely the derivation of the acceleration given in appendix C. The desired transfer function expressing the angle of attack is given as

$$\frac{\alpha}{\delta}(p) = \frac{K_g(T_r p+1)}{(T_a^2 p^2+2\zeta_a T_a p+1)} \tag{D1}$$

In response to a step of surface deflection δ_L

$$\alpha(p) = \frac{K_g\delta_L(T_r p+1)}{p(T_a^2 p^2+2\zeta_a T_a p+1)} = \frac{K_g T_r \delta_L\left(p+\frac{1}{T_r}\right)}{T_a^2 p[(p+\sigma_a)^2+\lambda_a^2]} \tag{D2}$$

the solution of which is

$$\alpha(t) = \frac{K_g T_r \delta_L}{T_a^2}\left[\frac{1}{T_r(\sigma_a^2+\lambda_a^2)} + \frac{\sqrt{\left(\frac{1}{T_r}-\sigma_a\right)^2+\lambda_a^2}}{\lambda_a\sqrt{\sigma_a^2+\lambda_a^2}} e^{-\sigma_a t}\sin(\lambda_a t+\varphi_1+\rho_1)\right] \tag{D3}$$

where

$$\varphi_1 = \tan^{-1}\frac{\lambda_a}{\frac{1}{T_r}-\sigma_a}$$

The first half period is represented by equation (D3) which can be written in the following form, again changing the sign of the second term as was explained for equation (C4)

$$\alpha(t) = c_o - c_1 e^{-\sigma_a t}\sin(\lambda_a t+\varphi_1+\rho_1) \tag{D4}$$

in which

$$c_o = K_g\delta_L$$

$$c_1 = \frac{K_g T_r \delta_L}{\lambda_a}\sqrt{\left(\frac{1}{T_r}-\sigma_a\right)^2+\lambda_a^2}\sqrt{\sigma_a^2+\lambda_a^2}$$

As an approximation, it is possible to show that for all these missiles $\lambda_a \gg \sigma_a$ and $1/T_r \gg \lambda_a \gg \sigma_a$ so that $c_1 \approx c_o$. Then

$$\alpha(t) \approx c_o - c_o e^{-\sigma_a t} \sin(\lambda_a t + \varphi_1' + \rho_1) \tag{D5}$$

$$\varphi_1' = \tan^{-1} \lambda_a T_r$$

For the second half period

$$\alpha(t) = c_o - c_1 e^{-\sigma_a t} \sin(\lambda_a t + \varphi_1 + \rho_1) -$$

$$2\left\{c_o - c_1 e^{-\sigma_a (t - t_{s1})} \sin[\lambda_a (t - t_{s1}) + \varphi_1 + \rho_1]\right\}$$

which simplifies to

$$\alpha(t) = -c_o - c_1 e^{-\sigma_a t} \sqrt{\eta^2 + \Omega^2} \sin(\lambda_a t + \varphi_1 + \rho_1 + \rho_2) \tag{D6}$$

in the manner as shown for equation (C6). The approximation $c_1 \approx c_o$ and $\varphi_1' \approx \varphi_1$ then gives

$$\alpha(t) \approx -c_o - c_o e^{-\sigma_a t} \sqrt{\eta^2 + \Omega^2} \sin(\lambda_a t + \varphi_1' + \rho_1 + \rho_2) \tag{D7}$$

The peak values of equations (D4) and (D6) during the first and second half periods will be defined to occur at t_{y1} and t_{y2}, respectively. The similarity of equation (D4) to equation (C4) gives a value of t_{y1} by analogy with the corresponding equation for t_{x1}

$$t_{y1} = \frac{n\pi - \varphi_1}{\lambda_a} \tag{D8}$$

Then, it can be shown that for $n = 1$

$$\alpha_{max} = c_o + c_1 e^{-\sigma_a t_{y1}} \frac{\lambda_a}{\sqrt{\sigma_a^2 + \lambda_a^2}} \tag{D9}$$

or

$$\alpha_{max} \approx c_o + c_o e^{-\sigma_a t_{y1}} \tag{D10}$$

For the second half period the same analogy between equations (D6) and (C6) may be used to write directly

$$t_{y2} = \frac{n\pi - \varphi_1 - \rho_2}{\lambda_a} \tag{D11}$$

Hence, for $n = 4$

$$\alpha_{max} = -c_o - c_1 e^{-\sigma_a t_{y2}\sqrt{\eta^2+\Omega^2}} \frac{\lambda_a}{\sqrt{\sigma_a{}^2+\lambda_a{}^2}} \tag{D12}$$

or,

$$\alpha_{max} \approx -c_o - c_o\sqrt{\eta^2+\Omega^2}\, e^{-\sigma_a t_{y2}} \tag{D13}$$

It might be noted that t_{y1} and t_{y2} are defined differently from t_{x1} and t_{x2}, respectively, although numerically they are equal because φ_1 and ψ_1 are nearly equal.

Numerical substitution of missile parameters then gives the following values, some of which have already been worked out in the development of the acceleration equations but are repeated here for convenience:

Parameter	Variable incidence	Canard	Tail aft control
c_o, deg	5.9	10.8	20.5
t_{y1}, sec	.247	.244	.244
t_{y2}, sec	.872	.865	.855
η	.606	.550	.638
Ω	2.99	3.42	2.76
ρ_1, deg	86.9	85.9	87.6
ρ_2, deg	78.6	80.9	77.0
φ_1', deg	-2.7	-.3	.4

The preceding values then give the following results for the time history and maximum values of the critical-surface angle of attack:

	Critical-surface angle of attack (deg)	
	Time history	Maximum value
Half period 1		
Variable incidence	$20.5 - 5.9e^{-0.691t} \sin (739t+84.2)$	25.5
Canard	$20.5 - 10.8e^{-0.917t} \sin (739t+85.6)$	29.1
Tail aft control	$20.5 - 20.5e^{-0.547t} \sin (739t+88.0)$	38.4
Half period 2		
Variable incidence	$-20.5 - 18.0e^{-0.691t} \sin (739t+162.8)$	-30.4
Canard	$-20.5 - 37.2e^{-0.917t} \sin (739t+166.5)$	-37.3
Tail aft control	$-20.5 - 58.3e^{-0.547t} \sin (739t+165.0)$	-57.0

APPENDIX E

OPTIMIZATION OF A PRACTICAL STABILIZATION SYSTEM

A practical stabilization system approaches the optimum system by causing the half periods of surface deflection to approach the values produced by an ideal stabilization system as given by equation (B4). Initially, the step $\overline{Z}_B$ signal causes the surface to deflect to its limit. The surface will remain at this limit until the negative feedback signals from θ and Z_M cause E_P and E_L, shown in figure 2, to become large enough to overcome the initial surface deflection. Hence, it is necessary to determine the manner in which they vary with time.

Lead-Network Limiter Signal E_L

From figure 2, it can be seen that

$$E_{LN}(p) = Y_L(Z_B - Z_M) = Y_L Z_B - Y_L Z_M \tag{E1}$$

For a step displacement of the beam of magnitude $\overline{Z}_B$, $Z_B(p) = \overline{Z}_B/p$ and $Z_M(p)$ is given by equation (A3). Then by substitution and separation into partial fractions,

$$E_{LN}(p) = K_2(\overline{Z}_B - a_0)\left(\frac{1}{p} + \frac{T_4-T_5}{1+T_5p}\right) - K_2a_1\left[\frac{T_4-T_5}{p} + \frac{1}{p^2} + \frac{-T_5(T_4-T_5)}{1+T_5p}\right] -$$

$$K_2a_2\left[\frac{-T_5(T_4-T_5)}{p} + \frac{T_4-T_5}{p^2} + \frac{1}{p^3} + \frac{T_5^2(T_4-T_5)}{1+T_5p}\right] -$$

$$K_2a_3\left[\frac{g_1+ih_1}{1+T_5p} + \frac{g_2+ih_2}{p-(-\sigma_a+i\lambda_a)}\right] - K_2\bar{a}_3\left[\frac{g_1-ih_1}{1+T_5p} + \frac{g_2-ih_2}{p-(-\sigma_a-i\lambda_a)}\right]$$

where

$$g_1 = \frac{(T_5-T_4)(\sigma_aT_5-1)}{(\sigma_aT_5-1)^2 + T_5^2\lambda_a^2} \qquad h_1 = \frac{(T_5-T_4)T_5\lambda_a}{(\sigma_aT_5-1)^2 + T_5^2\lambda_a^2}$$

$$g_2 = \frac{(1-\sigma_aT_4)(1-\sigma_aT_5) + T_4T_5\lambda_a^2}{(1-\sigma_aT_5)^2 + T_5^2\lambda_a^2} \qquad h_2 = \frac{T_4\lambda_a(1-T_5\sigma_a) - T_5\lambda_a(1-T_4\sigma_a)}{(1-T_5\sigma_a)^2 + T_5^2\lambda_a^2}$$

The solution for $E_{LN}(t)$ can be reduced to

[redacted]

$$E_{LN} = K_2 [l_0 + l_1 t + l_2 t^2 + l_3 e^{-t/T_5} + l_4 e^{-\sigma_a t} \sin (\lambda_a t - \epsilon_2)] \qquad (E2)$$

in which

$$l_0 = \bar{Z}_B - a_0 - a_1(T_4 - T_5) + a_2 T_5 (T_4 - T_5)$$

$$l_1 = - [a_1 + a_2(T_4 - T_5)]$$

$$l_2 = - \frac{a_2}{2}$$

$$l_3 = \frac{1}{T_5} [(\bar{Z}_B - a_0)(T_4 - T_5) + a_1 T_5 (T_4 - T_5) - a_2 T_5^2 (T_4 - T_5) - 2(a_{3R} g_1 - a_{3I} h_1)]$$

$$l_4 = 2 \sqrt{f_1^2 + f_2^2}$$

$$f_1 = a_{3R} g_2 - a_{3I} h_2$$

$$f_2 = a_{3I} g_2 + a_{3R} h_2$$

$$\epsilon_2 = \tan^{-1} \frac{f_1}{f_2}$$

Numerical evaluation shows that many of the above terms are negligible. Typical values of stabilization parameters of $k_2 = 1.19$, $T_4 = 0.43$, and $T_5 = 0.09$, together with the parameters given in table II, show that

$$E_{LN} \approx K_2 [l_0' + l_1' t + l_2 t^2 + l_3' e^{-t/T_5} + l_4 e^{-\sigma_a t} \sin (\lambda_a t - \epsilon_2)] \qquad (E3)$$

where

$$l_0' = \bar{Z}_B + a_2 T_5 (T_4 - T_5)$$

$$l_1' = -a_2 (T_4 - T_5)$$

$$l_3' = \frac{1}{T_5} (T_4 - T_5)(\bar{Z}_B - a_2 T_5^2)$$

A typical equation for the variable-incidence missile evaluated from equation (E3) gives

$$E_{LN} \approx 1.19 [109.8 - 109.5t - 161t^2 + 367e^{-11.1t} + 3.59e^{-0.681t} \sin(739t - 68.2)] \qquad (E4)$$

The signal E_{LN} is then fed to a limiter (representing the saturation of the radar receiver and amplifier) set for a value of voltage corresponding to a 25-foot positional error. This means that the limiter output E_L is equal to $25k_2$ for all values of time for which $E_{LN} \geq 25k_2$ and that $E_L = E_{LN}$ whenever $E_{LN} \leq 25k_2$. For example, for the variable-incidence

missile, linear operation obeying equation (E3) occurs for times greater than 0.48 second.

Pitch-Angle Feedback Signal, E_p

The feedback signal E_p can be determined from the response to the limit surface deflection. From figure 2, it can be seen that

$$\frac{E_p}{\delta}(p) = Y_\theta Y_p = \frac{K_3(1+T_m p)(1+T_2 p)}{VT_s^2(T_a^2 p^2+2\zeta_a T_a p+1)(1+T_3 p)} \tag{E5}$$

For $\delta(p) = \delta_L/p$, the response is

$$E_p(p) = \frac{\delta_L T_m K_3 T_2 \left(p+\frac{1}{T_m}\right)\left(p+\frac{1}{T_2}\right)}{VT_s^2 T_a^2 T_3\, p\left(p+\frac{1}{T_3}\right)(p^2+2\sigma_a p+\sigma_a^2+\lambda_a^2)} \tag{E6}$$

the solution of which is

$$E_p(t) = K_p[R_o + R_1 e^{-t/T_3} + R_2 e^{(-\sigma_a+i\lambda_a)t} + \bar{R}_2 e^{(-\sigma_a-i\lambda_a)t}]$$

$$= K_p[R_o + R_1 e^{-t/T_3} + R_3 e^{-\sigma_a t} \sin(\lambda_a t - \epsilon_3)] \tag{E7}$$

where

$$K_p = \frac{\delta_L T_m K_3 T_2}{VT_s^2 T_a^2 T_3}$$

$$R_o \approx \frac{T_3}{T_m T_2 \lambda_a^2}$$

$$R_1 \approx \frac{\frac{1}{T_M}+\frac{1}{T_2}-\frac{1}{T_3}-\frac{T_3}{T_m T_2}}{\left(\frac{1}{T_3}\right)^2-\frac{2\sigma_a}{T_3}+\lambda_a^2}$$

$$R_2 = \frac{d_1 + id_2}{2\lambda_a(d_3+id_4)}$$

$$R_3 = 2\sqrt{d_5^2 + d_6^2}$$

$$\epsilon_3 = \tan^{-1}\frac{d_5}{d_6}$$

$$d_1 \approx \frac{1}{T_m T_2} - \sigma_a\left(\frac{1}{T_m}+\frac{1}{T_2}\right) - \lambda_a^2$$

$$d_2 = \lambda_a\left(\frac{1}{T_m}+\frac{1}{T_2}\right) - 2\sigma_a\lambda_a$$

$$d_3 = 2\sigma_a\lambda_a - \frac{\lambda_a}{T_3}$$

$$d_4 \approx -\lambda_a^2 - \frac{\sigma_a}{T_3}$$

$$d_5 = \frac{d_1 d_3 + d_2 d_4}{2\lambda_a(d_3^2+d_4^2)}$$

$$d_6 = \frac{d_2 d_3 - d_1 d_4}{2\lambda_a(d_3^2+d_4^2)}$$

Numerical evaluation for all the missiles shows that to a good approximation

$$E_p(t) \approx K_p [R_o + R_s e^{-\sigma_a t} \sin (\lambda_a t - \epsilon_s)] \tag{E8}$$

For the variable-incidence missile, using typical values of $T_2 = 0.07$, $T_3 = 0.7$, and $k_s = 44.2$,

$$E_p \approx 5.36 + 8.72 e^{-0.681 t} \sin (739t - 46.7) \tag{E9}$$

Switching Time, t_{s1}

It is now possible to find the half-period time of the surface deflection. As described in the text the determination is made by opening the loop between Y_s and Y_θ, by applying a step deflection to the surface, and by calculating the return signal at the output of Y_s. Using an ideal servo as an approximation, the surface deflection will be

$$\delta(t) = \frac{1}{K_1} [E_L(t) - E_p(t)] \tag{E10}$$

Examination of equation (E10) shows that for small values of time $\delta(t)$ is larger than its limited value and hence must remain at this limit. At a later time, however, the E_L signal decreases sufficiently to allow $\delta(t)$ to begin operation in the linear range. Switching to the opposite limit occurs in a relatively short time so that the approximation to a square wave is good. The exact expressions for the feedback signals E_L and E_p are somewhat lengthy, which would make it difficult to solve for t from equation (E10). A good approximation can be made by using

$$E_L(t) \approx K_2[l_o' + l_1' t + l_2 t^2]$$

$$E_p(t) \approx K_p R_o$$

Then equation (E10) becomes

$$\delta_L K_1 \approx (K_2 l_o' - K_p R_o) + K_2 l_1' t + K_2 l_2 t^2$$

and the solution for the half period is

$$t_{s1} \approx \frac{-l_1'}{2l_2} + \frac{1}{2l_2} \sqrt{(l_1')^2 - 4l_2 \left(l_o' - \frac{K_p R_o}{K_2} - \frac{\delta_L K_1}{K_2} \right)} \tag{E11}$$

Evaluation for the variable-incidence missile using $K_1 = 0.02$ and the constants already presented shows that

$$t_{s1} \approx -0.34 + 0.0031\sqrt{12{,}000 + 644(109.8 - 4.5 - 10.7)}$$

$$t_{s1} \approx 0.50$$

which is close to the optimum value of 0.598. This means that the assumed constants would produce a nearly optimum system.

If higher accuracy is desirable for values of t_{s1}, an iterative process utilizing equations (E2), (E7), and (E11) may be employed. The effect of the neglected terms is to add a small additional term in the second parenthesis of equation (E11). For the variable-incidence missile, for example, the neglected terms amount to only 0.24.

It is possible to determine the relative importance of the various parameters controlling the switching time. A comparison of equations (E3) and (E8) with equation (E11) reveals that the feedback signal E_L is involved in every term of the t_{s1} equation while the signal E_p occurs in only the middle term of the second parenthesis. It is shown above that this term is small compared to the remaining terms in the parenthesis although not completely negligible. The remainder of the equation involves only the constants l_0', l_1', and l_2. Definitions of these quantities show that for a given $\bar{Z}_B$ and a given a_2, which can be seen from appendix A to represent the steady acceleration, the parameters l_0', l_1', and l_2 are functions of only the lead-network constants T_4 and T_5 and hence the missile response in reaching the beam is controlled primarily by these two time constants.

APPENDIX F

MISSILE RESPONSE TO A STEP CRITICAL-SURFACE ANGLE OF ATTACK

A step-displacement critical-surface angle of attack can be developed only by the variable-incidence and canard missiles since this critical angle is $(\alpha+\delta)$. The critical-surface angle for the tail-aft-control missile is α which cannot be developed rapidly enough to approach a step function. The transfer function relating missile position and critical-surface angle can be found from the relation

$$\frac{Z_M}{\alpha+\delta} = \frac{Z_M}{\delta} \times \frac{\delta}{\alpha+\delta} \tag{F1}$$

By definition, $Y_\alpha = \alpha(p)/\delta(p)$ so that

$$\frac{\delta}{\alpha+\delta}(p) = \frac{1}{1+Y_\alpha} = \frac{T_a^2p^2 + 2\zeta_aT_ap + 1}{T_a^2p^2 + (2\zeta_aT_a+K_gT_r)p + (1+K_g)} \tag{F2}$$

where Y_α has been given in the section on missile transfer functions. Carrying out the operation of equation (F1) by multiplying equation (F2) by (A1) and solving for Z_M in response to a step displacement of the critical angle $(\alpha+\delta)_L$,

$$Z_M = \frac{(\alpha+\delta)_L}{T_s^2(1+K_g)} \times \frac{T_b^2p^2 + 2\zeta_bT_bp + 1}{p^3\left[\left(\frac{T_a^2}{1+K_g}\right)p^2 + \left(\frac{2\zeta_aT_a+K_gT_r}{1+K_g}\right)p + 1\right]}$$

$$= \frac{(\alpha+\delta)_L}{T_s^2(1+K_g)} \times \frac{T_b^2p^2 + 2\zeta_bT_bp + 1}{p^3(T_{a1}^2p^2 + 2\zeta_{a1}T_{a1}p + 1)} \tag{F3}$$

It will be noticed that this equation is in the form of equation (A2) for the surface-deflection-limiter study and hence the solution developed in equation (A4) may be used by simply replacing δ_L, T_a, ζ_a, σ_a, and λ_a by $(\alpha+\delta)_L/(1+K_g)$, T_{a1}, ζ_{a1}, σ_{a1}, and λ_{a1}, respectively. The latter symbols can be written in terms of the former symbols as

$$T_{a1} = \frac{T_a}{\sqrt{1+K_g}}$$

$$\zeta_{a1} = \frac{\zeta_a}{\sqrt{1+K_g}} + \frac{K_gT_r}{2T_a\sqrt{1+K_g}}$$

$$\sigma_{a1} = \sigma_a + \frac{K_g T_r}{2T_a^2}$$

$$\lambda_{a1}^2 = \lambda_a^2 + \frac{K_g}{T_a^2} - \frac{K_g^2 T_r^2}{4T_a^4} - \frac{K_g T_r \sigma_a}{T_a^2}$$

The evaluation of these parameters using values given in table II is shown below for the variable-incidence and canard missiles:

Missile	T_{a1}	ζ_{a1}	σ_{a1}	λ_{a1}
Variable incidence	0.0654	0.0372	0.5697	15.27
Canard	.0534	.0470	.8811	18.70

The resultant time histories as evaluated by equation (A4) then gives:

Variable incidence $Z_M(t) = -0.393 - 0.79t + 161t^2 + 0.399e^{-0.57t}\cos(875t-9.5)$

Canard $Z_M(t) = -0.715 - 1.37t + 161t^2 + 0.722e^{-0.88t}\cos(1072t-8.4)$

Again, it may be seen that the missile response is approximated by the t^2 term or

$$Z_M(t) \approx \left[\frac{(\alpha+\delta)_L}{2(1+K_g)T_s^2}\right] t^2 \qquad (F4)$$

This equation can be simplified further. From equations (A7) and (A9), it is easy to show that

$$(\alpha+\delta)_L = ngT_s^2\left(1 - \frac{M_\delta}{M_\alpha}\right)$$

Also, using the definition of K_g given in the section on missile transfer functions, the factor $(1+K_g)$ can be shown to be approximated by

$$1 + K_g \approx 1 - \frac{M_\delta}{M_\alpha}$$

Hence, the response of equation (F4) becomes

$$Z_M(t) \approx \frac{ng}{2} t^2 \qquad (F5)$$

REFERENCES

1. Stone, H. N.: A Preliminary Investigation of the Merits of Wing Control or Tail Control in Pitch for a Target-Seeking Missile at Supersonic Speed. Curtiss-Wright Rep. R-47-26, Feb. 24, 1947.

2. Daggett, M. D., Jr.: An Investigation of Controllable Wing Versus Controllable Tail for the Control of Pilotless Aircraft. McDonnell Aircraft Rep. 577, March 3, 1947.

3. Stone, H. N., and Laster, W. R.: A Further Investigation of the Merits of Wing Control or Tail Control in Pitch for a Target-Seeking Missile at Supersonic Speed. Curtiss-Wright Rep. R-47-34, May 16, 1947.

4. Hunter, M. W., and Delameter, H. D.: The Aerodynamic Design and Testing of the Sparrow Missile. Douglas Rep. SM-13563, Nov. 4, 1949.

5. Anon: Sparrow XAAM-N-2 Pilotless Aircraft. Summary Report on Task 9A, Development of Missile Control System. Sperry Gyroscope Co., Inc., Rep. 5256-2191, Apr. 1949, pp. 119-131.

TABLE I.- SUMMARY OF MASS, GEOMETRIC, AND AERODYNAMIC CHARACTERISTICS OF THE THREE MISSILES

Lift ratio	0.50	0.10	−0.24
Missile / Parameter	Variable incidence	Canard	Conventional tail aft control
m, slugs	6.67	6.67	6.67
I_y, slug ft^2	41	41	41
S_f, ft^2	2.61	.86	1.49
S_r, ft^2	1.14	2.97	.90
l_f, ft	.20	3.69	.06
l_r, ft	4.56	3.22	4.70
L_α, lb/rad	10,300	10,320	7,450
L_δ, lb/rad	4,270	1,270	2,460
M_α, ft lb/rad	−6,800	−6,800	−6,800
M_δ, ft lb/rad	2,760	7,530	−11,560
$M_{\dot{\theta}}$, ft lb sec/rad	−26.4	−43.7	−22.5
$M_{\dot{\alpha}}$, ft lb sec/rad	−6.3	−7.5	−5.0
δ_L, rad	±.255	±.170	∓.211
$\left(\frac{\alpha}{\delta}\right)_{trim} \approx -\frac{M_\delta}{M_\alpha}$	.406	1.107	−1.700

NOTE: The body common to all three missiles was assumed to be 10.5 feet long, 8 inches in diameter, and with an ogival nose 4 feet in length. All plan forms have 30° semivertex angles. The controls are all-movable surfaces and the tails are interdigitated.

TABLE II.— SUMMARY OF MISSILE AERODYNAMIC AND STABILIZATION PARAMETERS

Parameter \ Figure No.	4(a)	4(b)	4(c)	5(a)	5(b)	5(c)	6(a)	6(b)	6(c)
T_a^2	0.006016	0.006007	0.006021	0.006016	0.006007	0.006021	0.006016	0.006007	0.006021
T_b^2	.003047	.000603	−.001454	.003047	.000603	−.001454	.003047	.000603	−.001454
T_8^2	.0007911	.0005284	−.0006547	.0007911	.0005284	−.0006547	.0007911	.0005284	−.0006547
T_m	.846	1.539	2.931	.846	1.539	2.931	.846	1.539	2.931
T_r	−.003611	−.000392	.000496	−.003611	−.000392	.000496	−.003611	−.000392	.000496
K_g	.404	1.103	−1.696	.404	1.103	−1.696	.404	1.103	−1.696
ζ_a	.0536	.0711	.0425	.0536	.0711	.0425	.0536	.0711	.0425
ζ_b	.0220	.0153	.01281	.0220	.0153	.01281	.0220	.0153	.01281
T_1	.025	.025	.025	.025	.025	.025	.025	.025	.025
T_2	.0721	.0721	.0721	.0721	.0721	.0721	.0721	.0721	.0721
T_3	.846	.846	1.000	.846	.846	.846	.846	.846	.846
T_4	.320	.370	.423	.395	.440	.530	.320	.395	.450
T_5	.0559	.0559	.0559	.0559	.0559	.0559	.0559	.0559	.0559
K_1	27.9	27.9	15.0	27.9	27.9	17.0	27.9	27.9	15.0
K_2	1.0	1.0	1.0	1.0	1.0	1.0	1.0	1.0	1.0
K_3	44.2	44.2	44.2	44.2	44.2	44.2	44.2	44.2	44.2

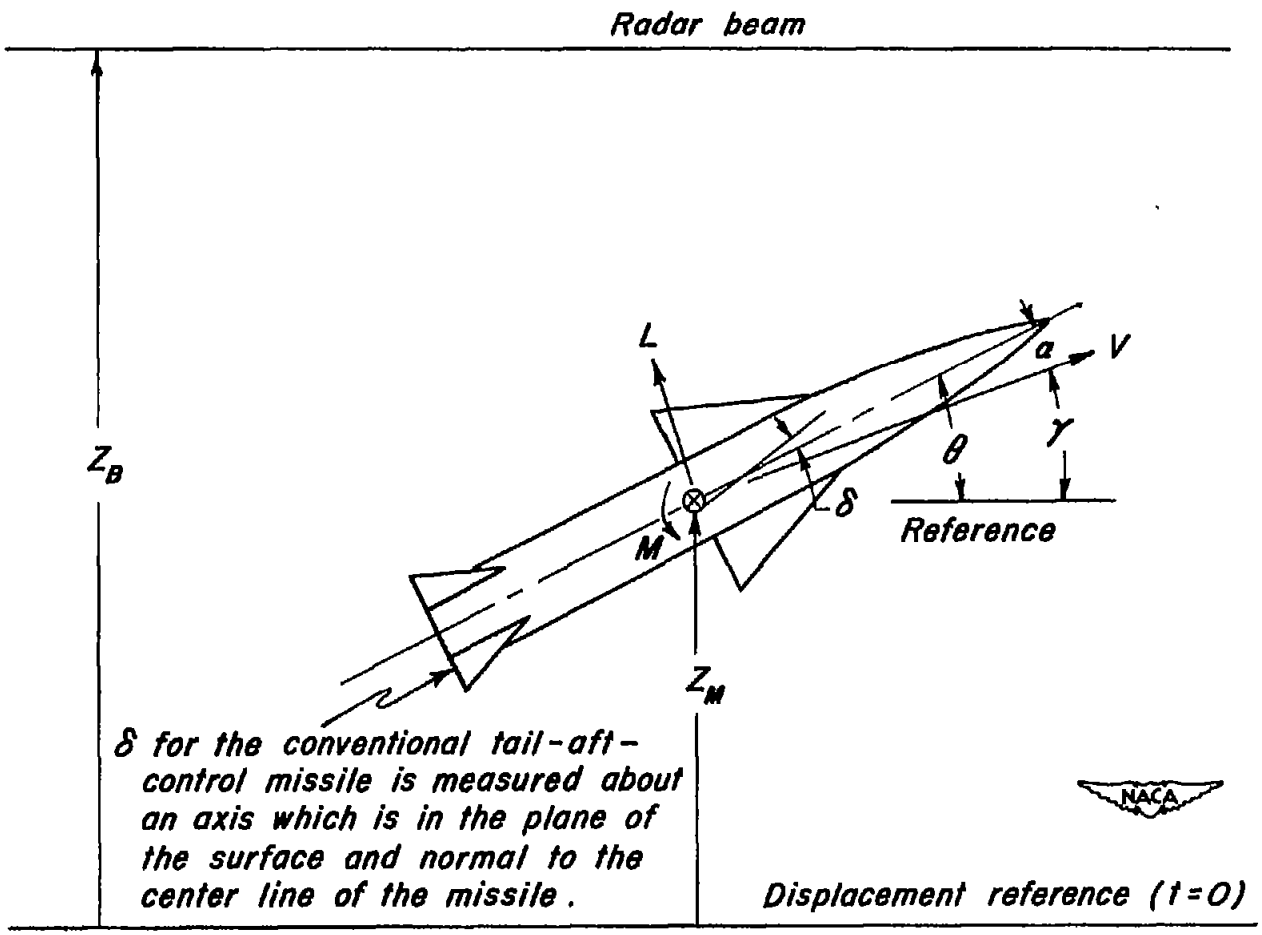

Figure 1.- System of axes, angular relationships, and displacements of missile and beam.

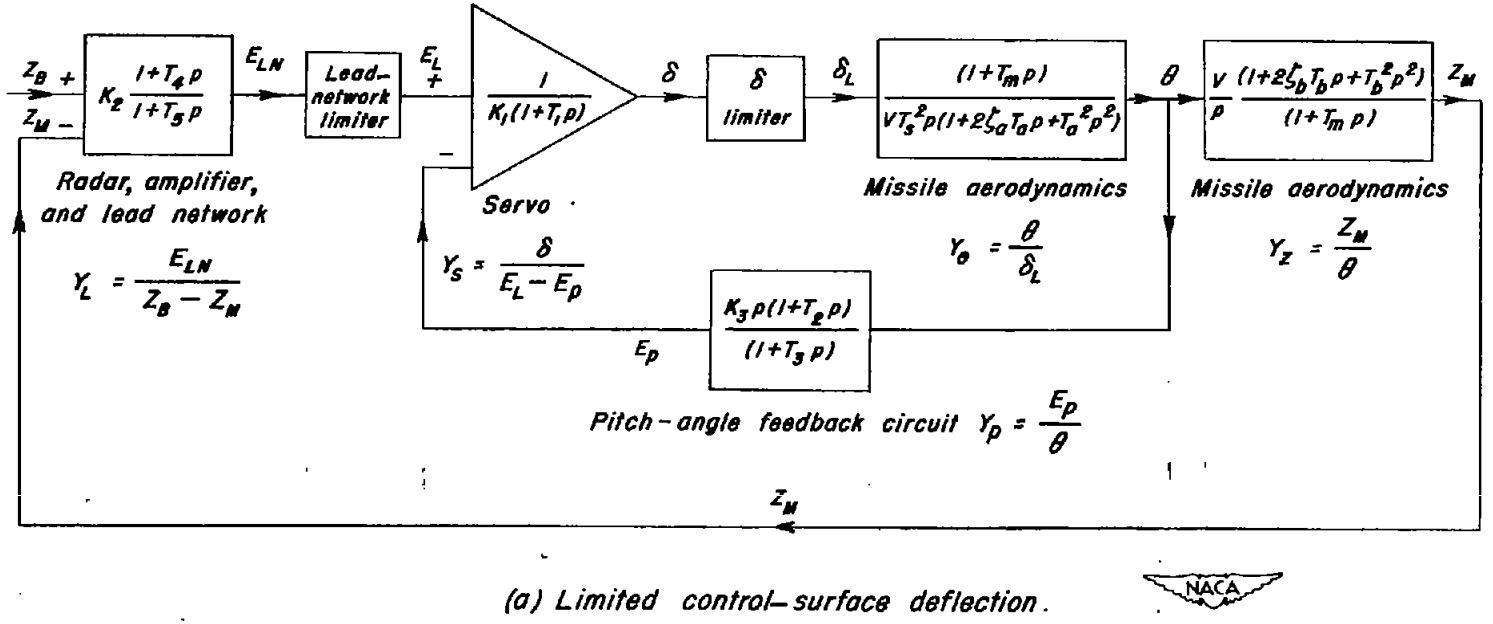

(a) Limited control-surface deflection.

Figure 2.- Block diagrams for control systems and missile.

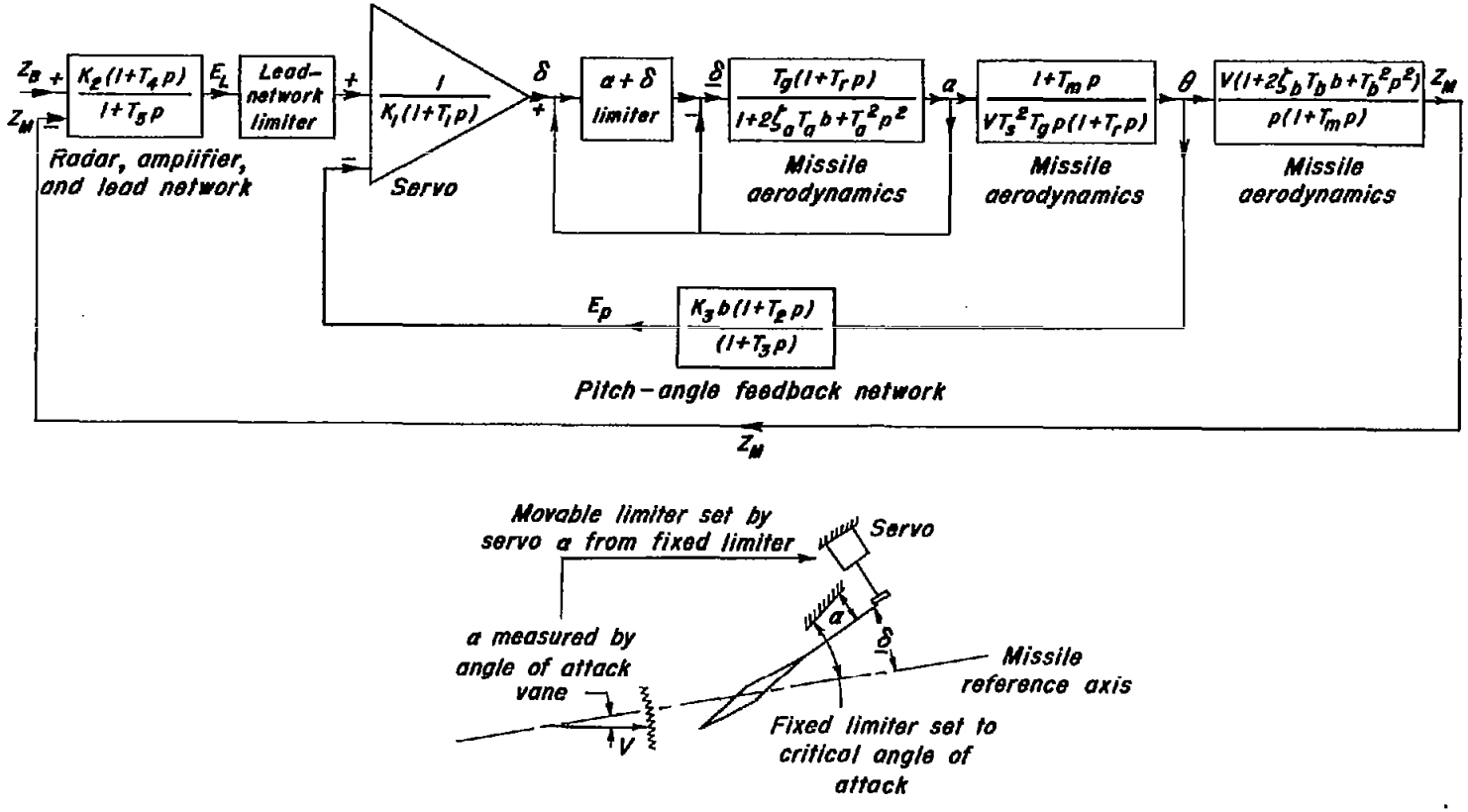

(b) Limited critical-surface angle of attack.

Figure 2.- Concluded.

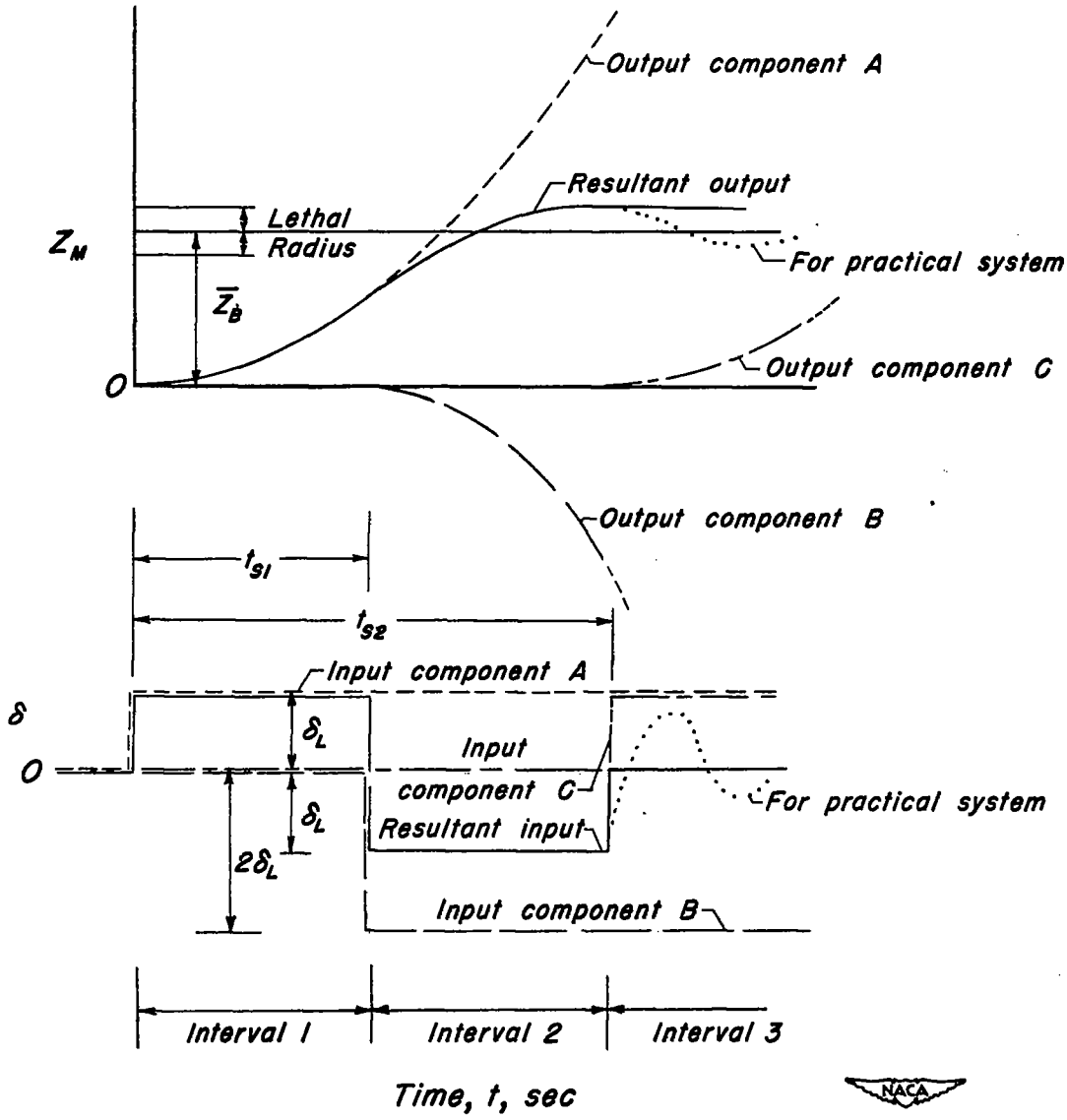

Figure 3.- Normal-displacement step response for an ideal system with limited control deflection.

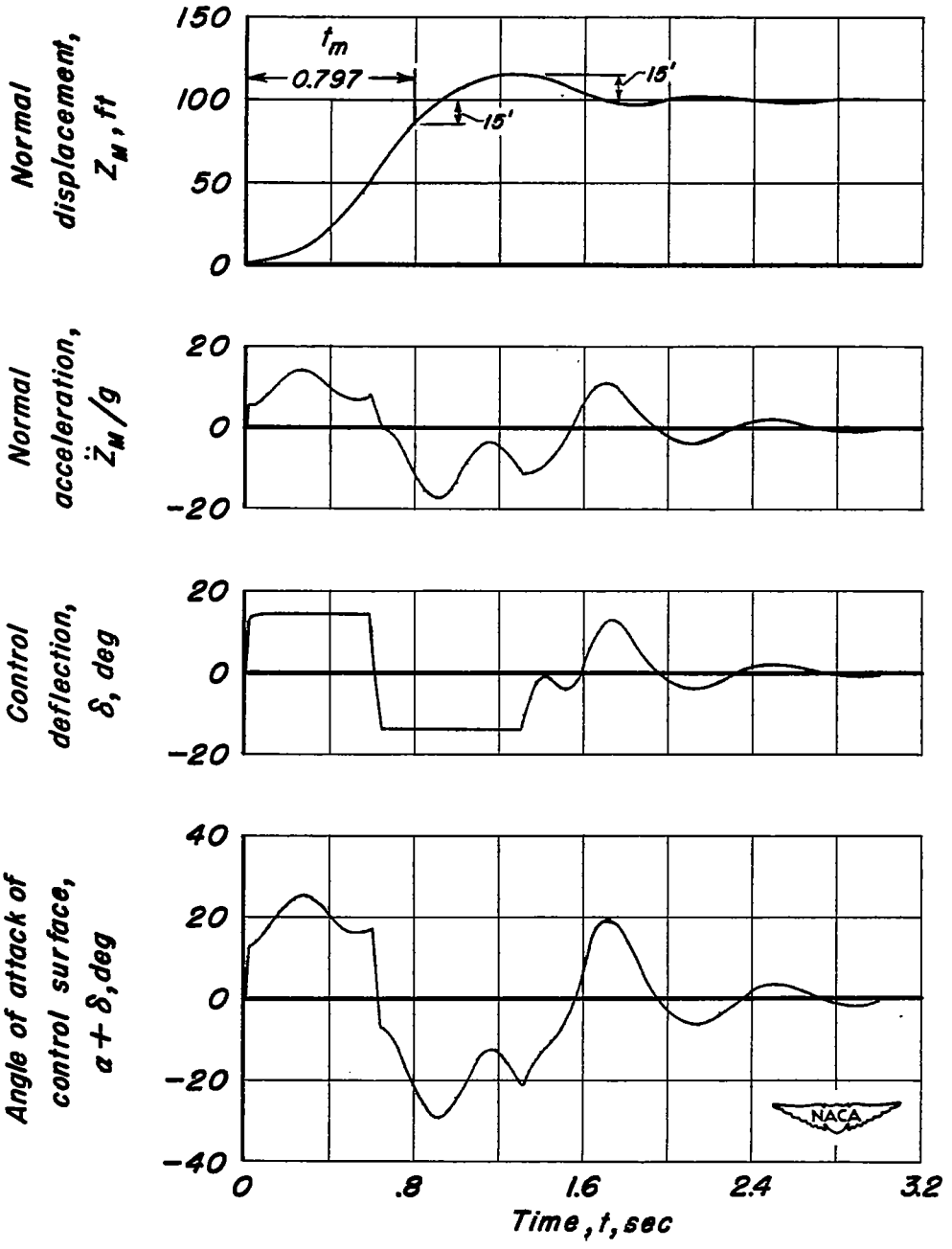

(a) Variable - incidence configuration.

Figure 4.- Transient characteristics for optimum normal - displacement response ; limited error and control deflection.

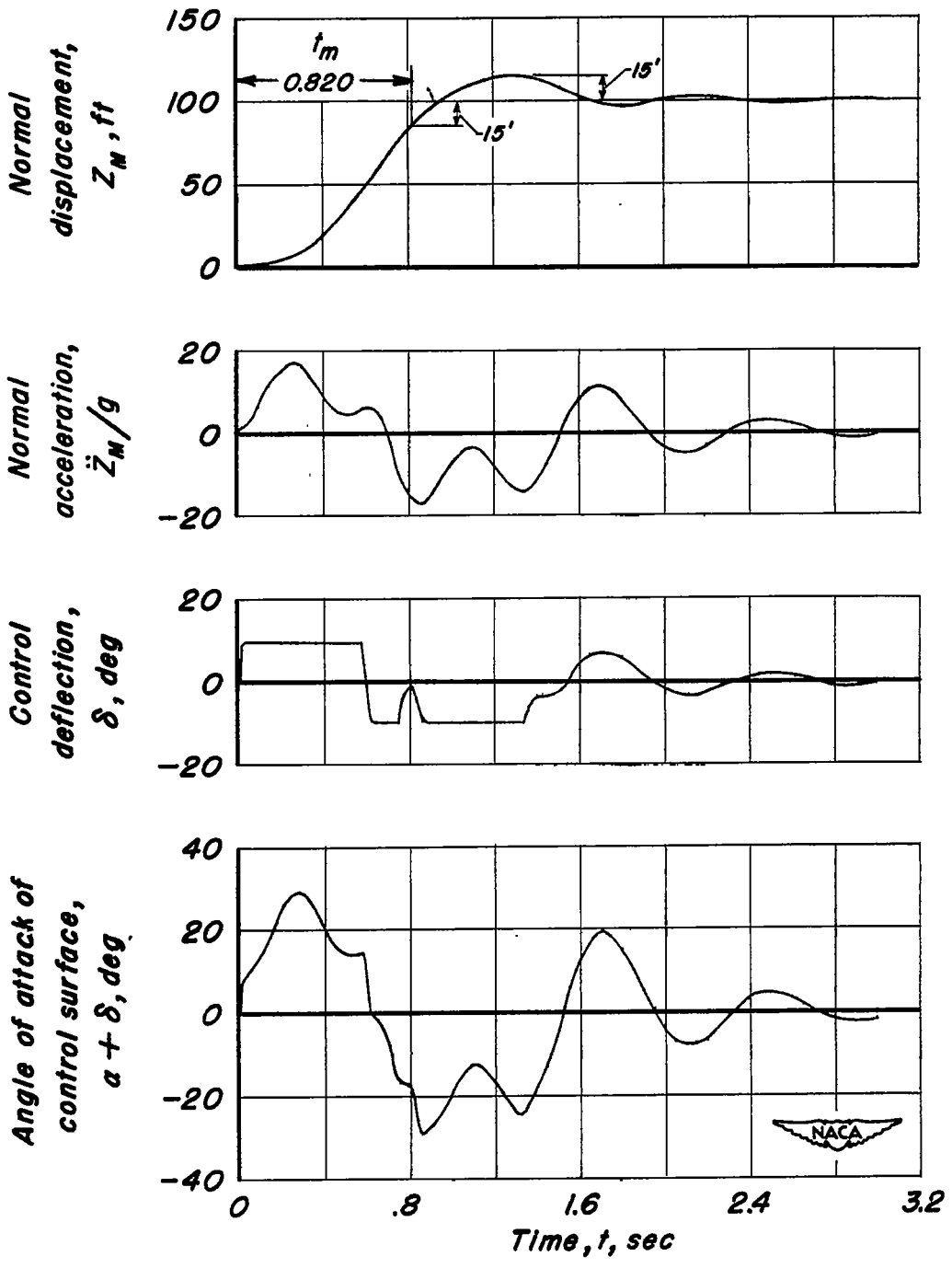

(b) Canard configuration.

Figure 4.- Continued.

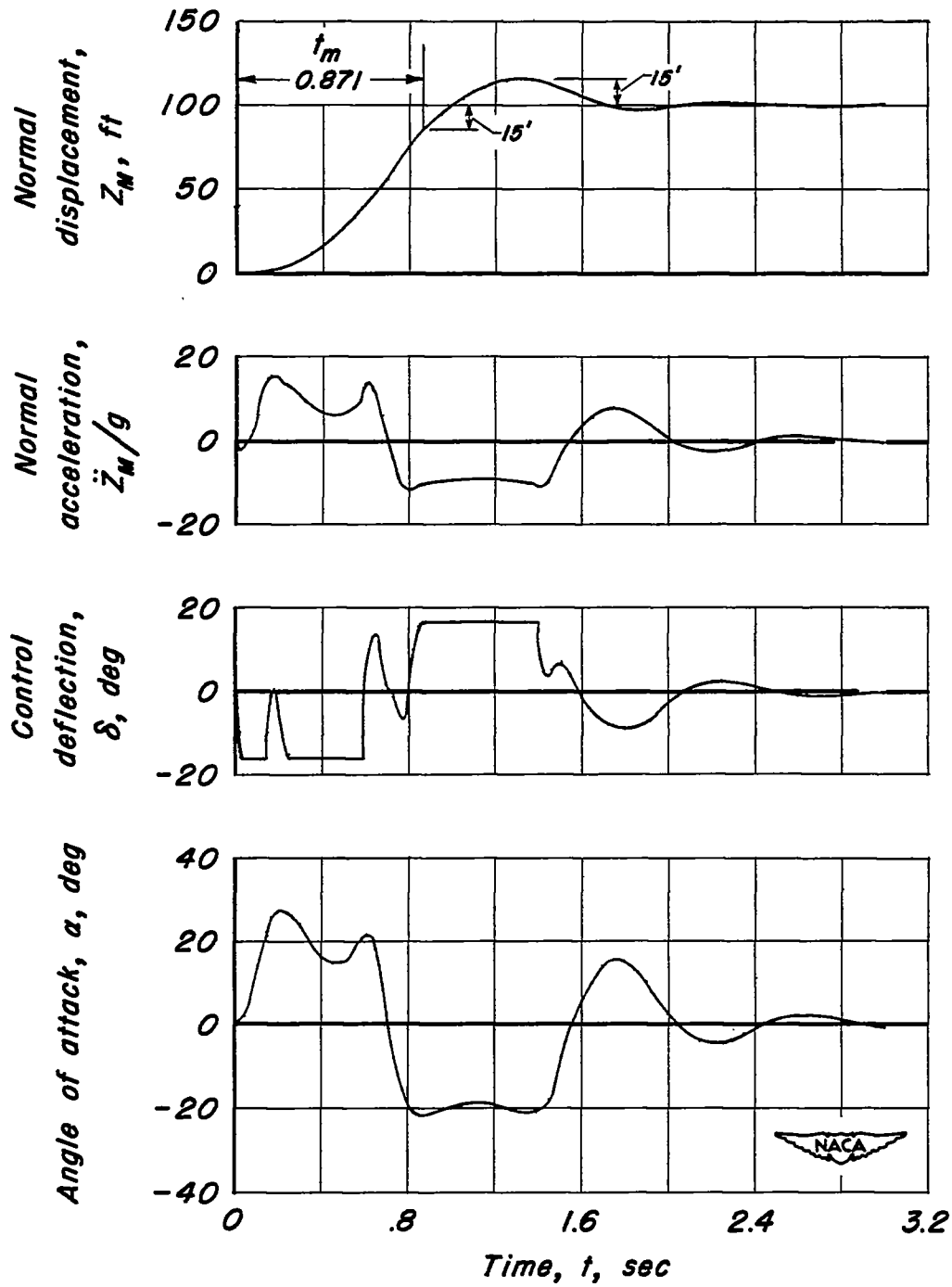

(c) Conventional tail - aft - control configuration.

Figure 4. - Concluded.

[redacted]

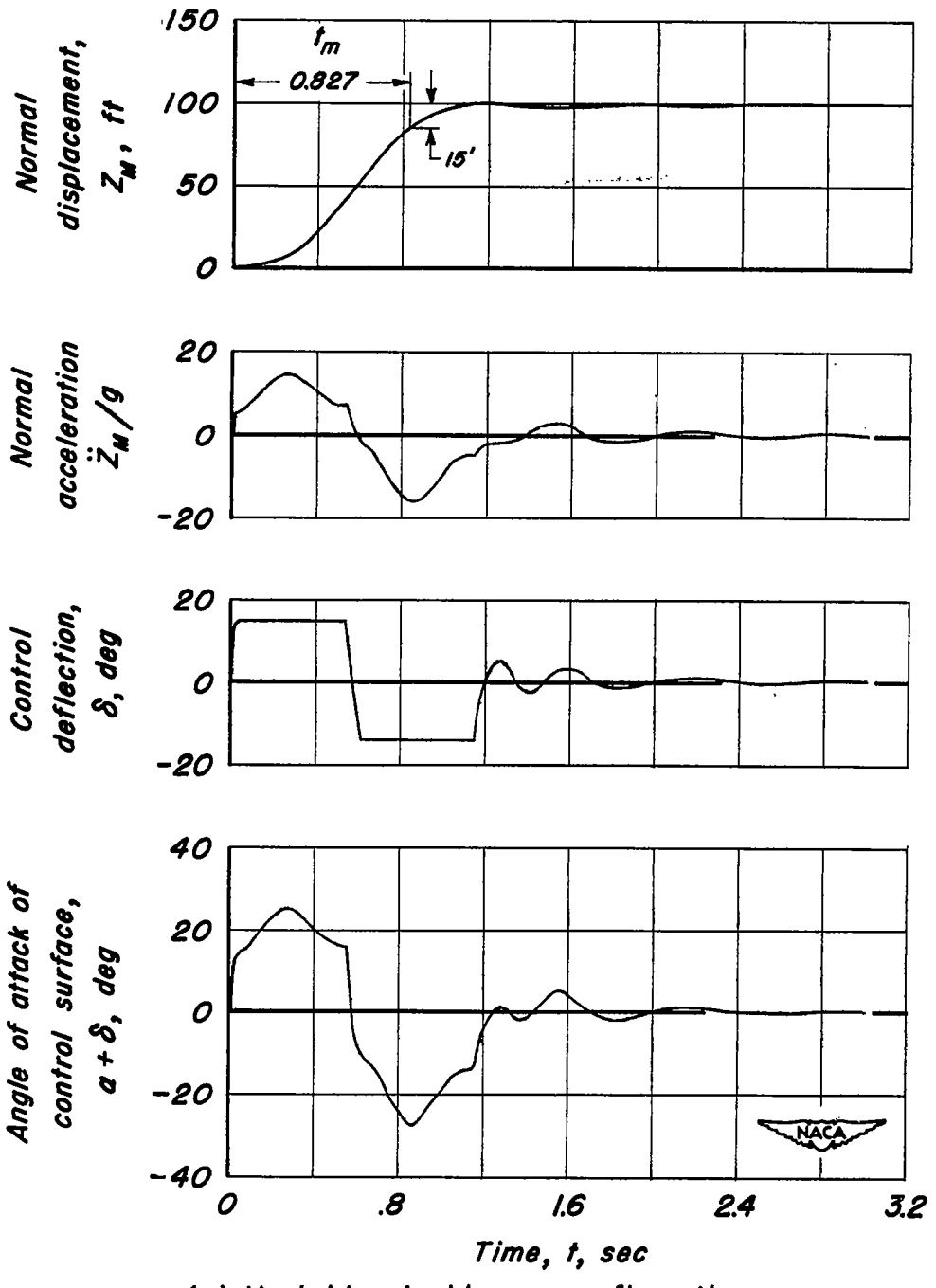

(a) Variable-incidence configuration.

Figure 5.—Transient characteristics for dead-beat normal-displacement response; limited error and control deflection.

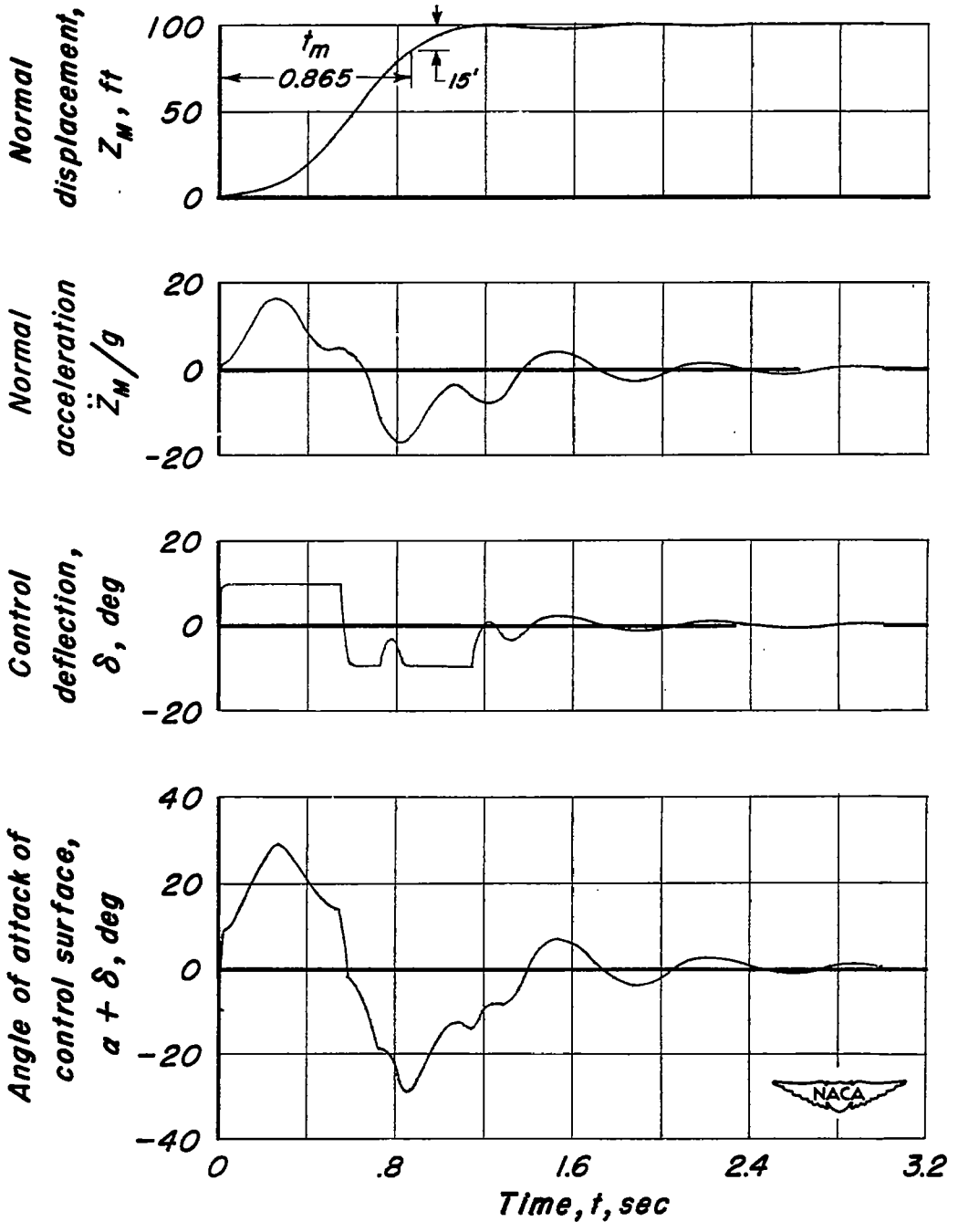

(b) Canard configuration.

Figure 5.- Continued.

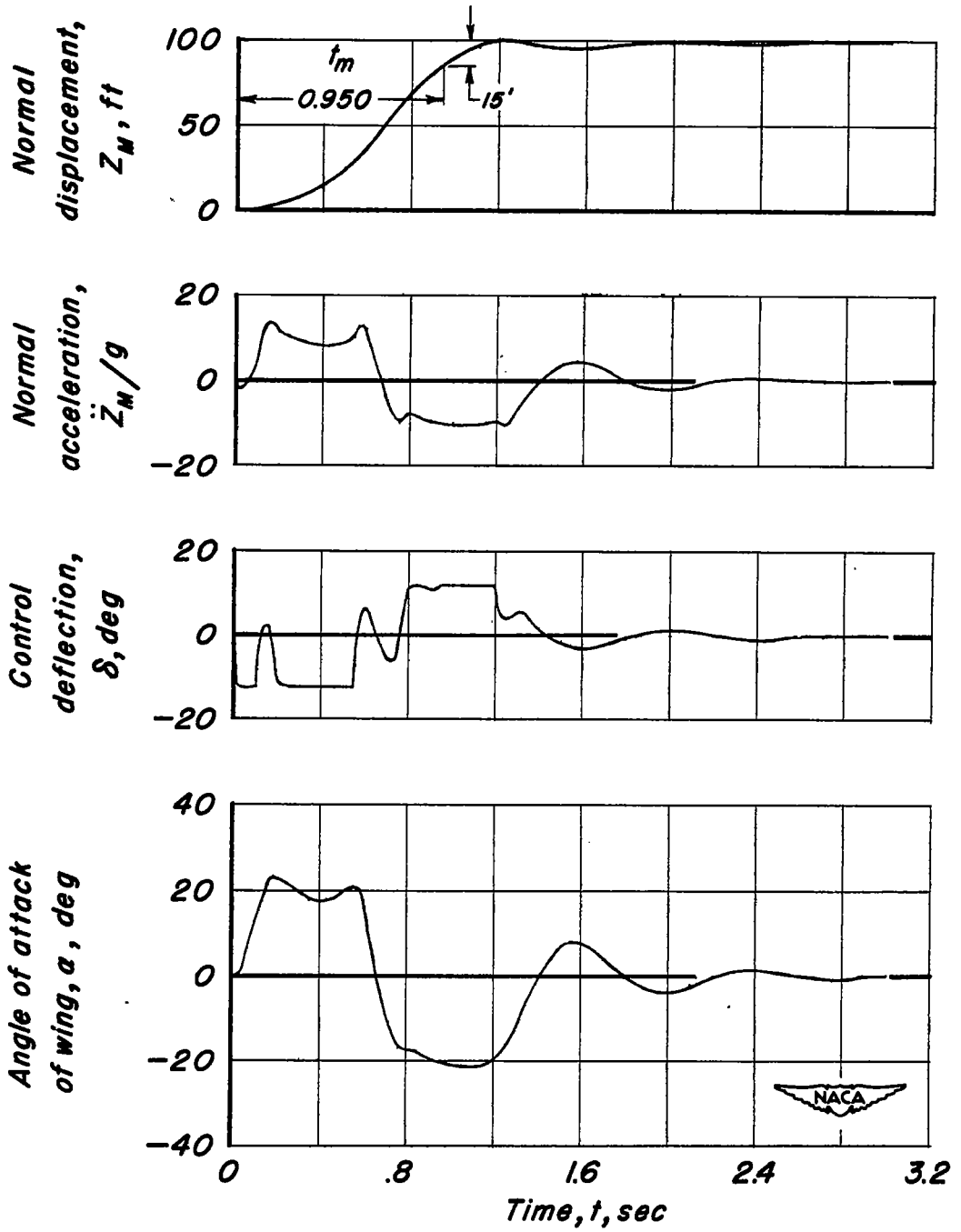

(c) Conventional tail-aft-control configuration.

Figure 5.- Concluded.

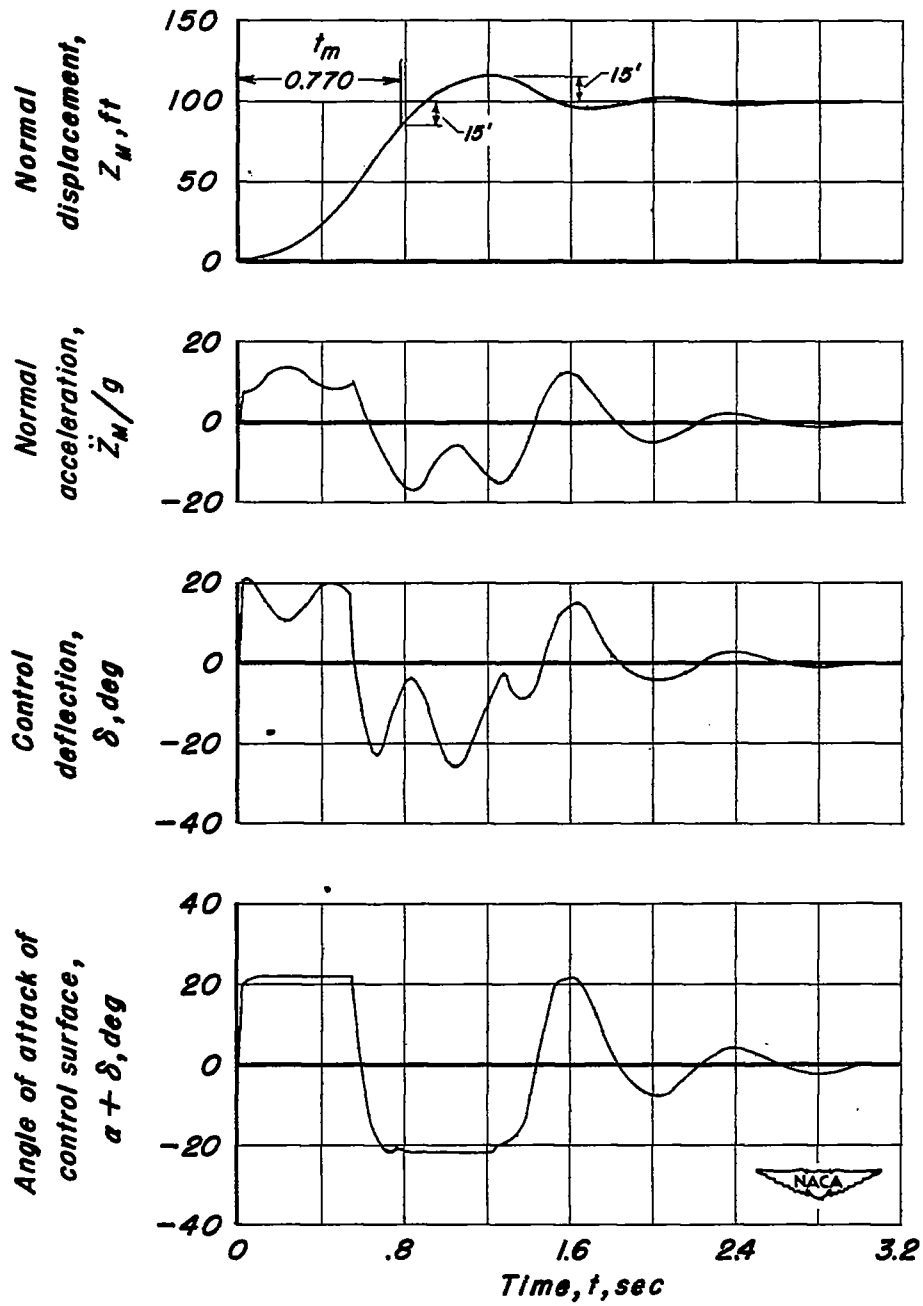

(a) Variable-incidence configuration.

Figure 6.- Transient characteristics for optimum normal-displacement response; limited error and critical surface angle of attack.

[redacted]

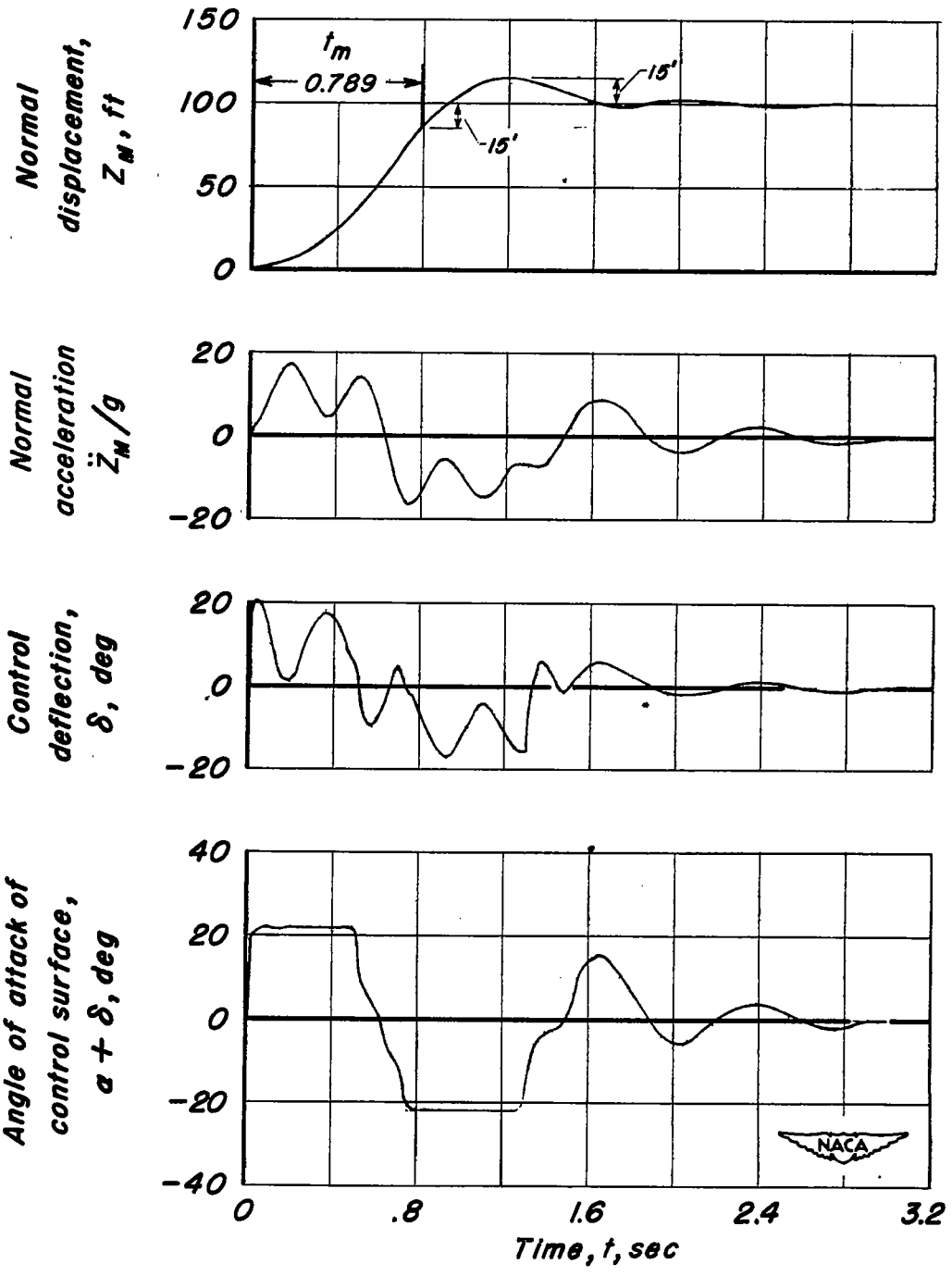

(b) Canard configuration.

Figure 6.- Continued.

[redacted]

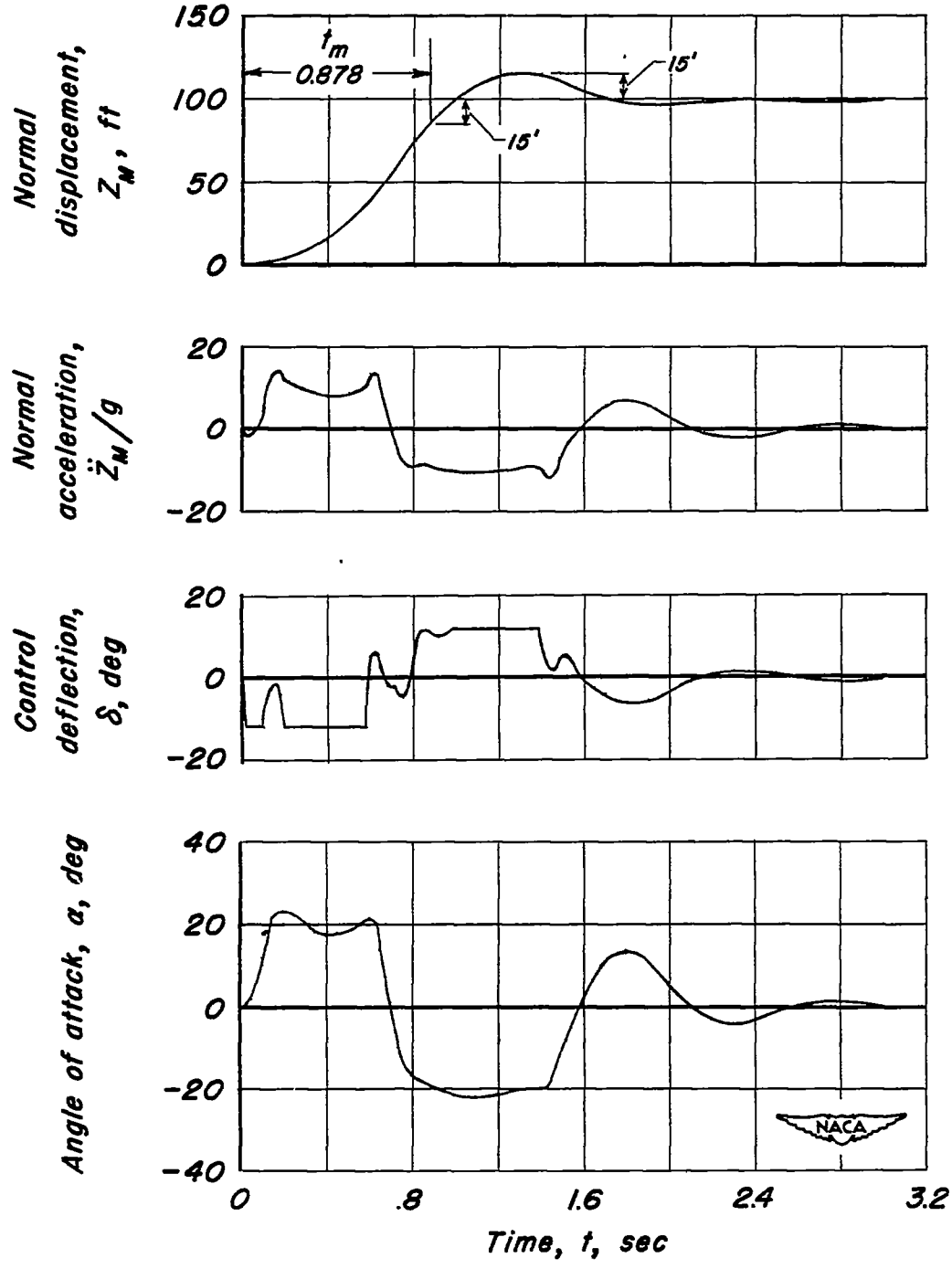

(c) Conventional tail-aft-control configuration.

Figure 6.- Concluded.

[redacted]

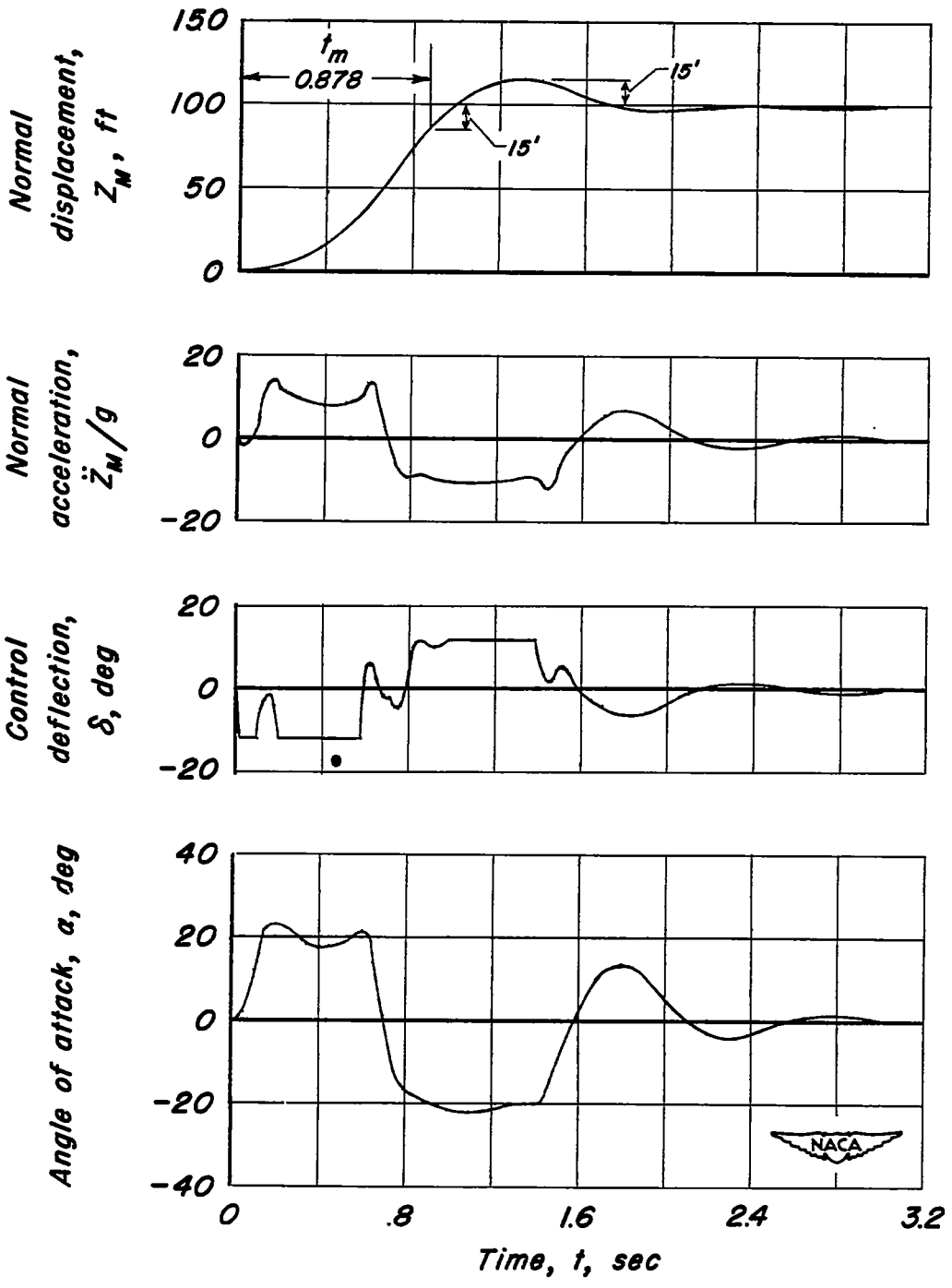

(c) Conventional tail-aft-control configuration.

Figure 6.- Concluded.

CONFIDENTIAL